UNIVERSITY OF HELSINKI REPORT SERIES IN PHYSICS

HU-P-D193

Mapping Conformal Field Theories on the Lattice

Jarno Rantaharju

Division of Elementary Particle Physics
Department of Physics
Faculty of Science
University of Helsinki
Helsinki, Finland

ACADEMIC DISSERTATION

To be presented, with the permission of the Faculty of Science of the University of Helsinki, for public criticism in the auditorium E204 at Physicum, Gustaf Hällströmin katu 2 A, Helsinki, on July 6th 2012 at 12 o'clock.

Helsinki 2012

ISBN 978-952-10-7088-4 (printed version)
ISSN 0356-0961
ISBN 978-952-10-7089-1 (pdf version)
http://ethesis.helsinki.fi
Helsinki University Print
Helsinki 2012

J. Rantaharju: Mapping Conformal Field Theories on the Lattice,
University of Helsinki, 2012, 53 pages,
University of Helsinki Report Series in Physics, HU-P-D193
ISSN 0356-0961
ISBN 978-952-10-7088-4 (printed version)
ISBN 978-952-10-7089-1 (pdf version)

Keywords: lattice field theory, conformal field theory, nonperturbative effects

Abstract

The Standard Model of particle physics and the modern understanding of physics at small length scales rests on the foundation of non-Abelian gauge theories. Mapping their behavior at large energies is important in understanding the Standard Model and in extending it to include a wider range of physical phenomena. There is a region in the parameter space of these models where the interaction strength runs to a constant at high energies. These conformal models are useful for explaining the masses of Standard Model particles trough the extended technicolor mechanism.

In this thesis I present studies of the conformal window using lattice simulations. This turns out to be a significant challenge in the study non-perturbative quantum physics. We have studied the phase structure of the SU(2) gauge theory coupled to fermions that transform in the fundamental or the adjoint representation of the symmetry group. We have found evidence of large discretization errors and studied them by constructing a Symanzik improved model. The running of the renormalized coupling is greatly affected by improvements in the model.

Using the Symanzik improved model we have studied the running of the coupling in the SU(2) gauge theory with fundamental fermions. The models behave as expected with 4 and 10 flavors of fermions. We were unable to distinguish between chirally broken and conformal behavior in the model with 6 fermions. In order to push further into large energy scales we have studied actions with NHYP and HEX smearing. This helps reduce the discretization effects and reduce the corrections in the Symanzik improvement. Using the improved HEX smeared action we have been able to run simulations at larger energy scales than before.

Acknowledgements

The research for this thesis was carried out at the Division of Elementary Particle Physics in the University of Helsinki. The numeric work was performed at the Center for Scientific Computing (CSC), at Jülich supercomputer center (JSC) and at EPCC, University of Edinburgh. I gratefully acknowledge the grant from Väisälä Foundation.

I would like to express my gratitude to my supervisor, Kari Rummukainen, for all his help and guidance. I would also like to thank Ari Hietanen, Kimmo Tuominen, Tuomas Karavirta and Anne Mykkänen for fruitful conversations and collaboration. I'm grateful to the pre-examiners of this thesis, Rainer Sommer and Claudio Pica, for carefully examining the manuscript and providing comments and corrections.

Finally, I would like to thank Maija, my family and friends for their support and encouragement, and my colleges for the friendly atmosphere.

Helsinki, May 2012

Jarno Rantaharju

Contents

List of Included Papers

I A. J. Hietanen, J. Rantaharju, K. Rummukainen and K. Tuominen,
"Spectrum of SU(2) lattice gauge theory with two adjoint Dirac flavours,"
JHEP **0905**, 025 (2009), [arXiv:0812.1467 [hep-lat]].

II T. Karavirta, A. Mykkanen, J. Rantaharju, K. Rummukainen and K. Tuominen,
"Nonperturbative improvement of SU(2) lattice gauge theory with adjoint or fundamental flavors,"
JHEP **1106**, 061 (2011), [arXiv:1101.0154 [hep-lat]].

III T. Karavirta, J. Rantaharju, K. Rummukainen and K. Tuominen,
"Exploring the conformal window: SU(2) gauge theory on the lattice,"
JHEP **1205**, 003 (2012), arXiv:1201.2037 [hep-lat].

Chapter 1

Introduction

For the past 60 years the Standard Model of particle physics has been very successful in describing the behavior of the most fundamental parts of our universe. With just a few particles and three basic interactions, it can describe the short scale behavior of almost everything and to an amazing accuracy. Richard Feynman compared the accuracy of QED, quantum electrodynamics, to measuring the width of North-America to a hairs width. On the other had it certainly misses some key aspects of the universe, like gravity, dark matter, the fact that there is more matter than antimatter, the expansion of the universe and so on. So naturally the Standard Model is not the final word. Rather physicists are constantly looking for possible corrections and additions to the model, that might explain the world a bit better. And of course we are constantly running experiments to see how far the model can be pushed, when will we see something that does not fit.

In this thesis I am especially interested in the masses of particles. In the Standard Model they are created trough an interaction with the Higgs boson, which is taken to be a fundamental particle. It is an odd particle in many ways. It has an interaction with itself that allows it to have a nonzero density in the vacuum. It is a scalar particle and has spin zero, unlike any other elementary particle. It's existence has not yet been verified experimentally, although the most recent results from the Large Hadron Collider seem to point to its existence at a certain mass range. However it is needed to explain the masses of the gauge bosons while keeping the theory mathematically well defined. In technicolor models it is suggested that the Higgs particle is actually a bound state of techniquarks that interact much like normal quarks with each other. There are some very specific requirements for an interaction that could create a suitable particle as a bound state.

Lattice simulations are a tool that has been developed to probe the strong interaction at relatively short length scales. Since its conception the lattice method has aspired to provide data at the physical range of fermion masses and interaction strength. In the last few years this has become possible thanks to improvements in the algorithms and the faster than exponential growth of computing power. In principal this has never been impossible, just very impractical. Simulating large enough lattices with strong enough interactions and small enough quark masses is still very time consuming, but with modern simulation algorithms and computers it can be done. This development has opened a way to study other possible field theories, with different interactions and quark contents. It is so far the only way to study these theories in their non-perturbative regions.

To understand how the Standard Model can be corrected it is important to understand how quantum field theories actually work. Thanks to the success of lattice simulations we can calculate prediction about measurable quantities, such as the masses of bound states, for many different kinds of theories and even with quite strong interactions, where perturbation theory does not work. The work that is presented in this thesis investigates two lattice gauge models

with different interactions. These models belong to a special class field theories that might be conformal or near conformal. Models like these could explain the masses of Standard Model particles while being quite similar to QCD themselves. In chapter 2 I introduce the reader to the relevant aspects of the Standard Model, the strong interaction and the Higgs mechanism and the ideas of technicolor models and conformal field theories. Chapter 3 introduces lattice simulations of field theories and way to make the standard algorithms more effective. Chapter 4 describes the methods of studying the conformality of a field theory and the models used in these studies. The bulk of my research is also described in the articles included in this thesis.

Chapter 2

The Standard Model

The Standard Model includes two fundamental interactions, governed by the strong and the electroweak symmetries. The electromagnetic and the weak forces are created when the Higgs boson breaks the electroweak symmetry. They are mediated by γ, W and Z bosons, the gauge fields of the symmetry. The strong interaction is mediated by gluons and affects the particles that have a color charge, quarks.

The strong interaction is described by QCD, quantum chromodynamics. It was first developed to explain the wide spectrum of hadrons and mesons found in particle accelerators. In addition to the protons, neutrons and pions that our everyday matter consists of, particle accelerators have found dozens of heavy hadrons and mesons that live only for short periods of time. In QCD, these particles are actually bound states of quarks and gluons and the strong force confines them inside these color-neutral bound states. Protons and neutrons are hadrons and the strong interactions bind them into nuclei. Since the force is so strong, the behavior of quarks is mainly controlled by it, the correction from the electroweak interaction are often too small to matter.

Leptons on the other hand are controlled only by the electroweak interaction. Since the interaction is weaker a lot of its effects can be calculated analytically. This means that the parameters of the electroweak sector are rather well known and provide the best tests for new expansions of the Standard Model. The new theory has to be compatible with all the precision measurements of the electroweak sector.

2.1 The strong interaction

The Standard Model theories are mathematically surprisingly simple. The essence of a quantum field theory is in the Lagrangian function, all the dynamics can be calculated from it. For QCD we can write it down as

$$L_{\mathrm{QCD}} = -\frac{1}{4} F^a_{\mu\nu} F^{a\mu\nu} + \sum_f \bar{\psi}_f \left(i\gamma^\mu D_\mu - m_f \right) \psi_f, \tag{2.1}$$

$$D_\mu = \partial_\mu - igA^a_\mu \lambda^a, \tag{2.2}$$

$$F^a_{\mu\nu} = [D_\mu, D_\nu] = \partial_\mu A^a_\nu - \partial_\nu A^a_\mu + g f^{abc} A^b A^c \tag{2.3}$$

There are two fundamental fields here, the quark ψ_f and the gauge fields A^a_μ. In nature there are six flavors of quarks, indexed with f. In addition each quark ψ is a vector of three colors, the charges of the theory, and 4 Dirac components. The gauge connections A^a_μ are vectors and are multiplied by the 3×3 Gell-Mann matrices λ^a, the generators of the SU(3) symmetry group. The f^{abc} are the structure constants of SU(3). Note that I use the Einstein

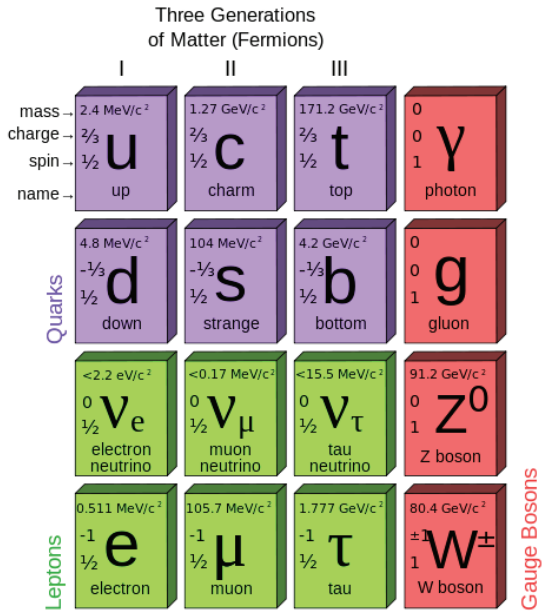

Figure 2.1: Particles in the Standard Model, with the Higgs boson still missing.

summation convention, repeated indexes are summed over. I will also often use the matrices $A_\mu = A^a_\mu \lambda^a$ instead of A^a_μ.

The Lagrangian is constructed so that it is invariant under both Lorentz transformations and the color transformation. Lorentz transformations are the coordinate transformations of special relativity, the model has to be invariant with respect to them, or the laws of nature would depend on the frame. The color transformation is given by

$$\begin{aligned}
\bar{\psi}(x) &\to \bar{\psi}(x) G^\dagger(x), \\
\psi(x) &\to G(x)\psi(x), \\
A_\mu(x) &\to G(x) A_\mu(x) G^\dagger(x) - \frac{1}{g} \left(\partial_\mu G(x)\right) G^\dagger(x).
\end{aligned}$$

Here $G(x)$ is an element of SU(3),

$$G(x) = e^{ic^a(x)\lambda^a}, \; G(x)^\dagger G(x) = 1, \; \det(G(x)) = 1.$$

The gauge symmetry encodes the interaction between the quarks and is naturally built into the model.

From this Lagrangian one could in principle calculate all the dynamics of the theory. The expectation value of a quantity Φ is given by

$$< \Phi >= \int d\psi d\bar{\psi} dA \; \Phi \; e^{i \int d^3x \, dt \, \mathcal{L}(\psi, \bar{\psi}, A)}.$$

There is of course no known way to directly calculate the integral. The parts that are quadratic in the fields are simple enough but the parts with more than two fields cannot be integrated. In perturbation theory one expands the interaction parts in terms of g, but since in QCD g is not very small and the expansion gets very complicated with higher orders of g, there are many things in QCD that cannot be calculated reliably from perturbation theory.

2.2 Symmetries of the QCD Lagrangian

The QCD Lagrangian is built so that it's symmetric with respect to gauge and Lorentz transformations. In addition it has some extra symmetries that affect the dynamics of the theory. One of these is the symmetry with respect to the U(1) transformation

$$\bar{\psi} \to \bar{\psi} e^{-i\phi},$$
$$\psi \to e^{i\phi}\psi.$$

To include the electromagnetic interaction to the theory this could be turned into a local gauge symmetry. Noethers theorem states any differentiable symmetry in the Lagrangian of a theory corresponds to a conservation law. The quantity that is conserved due to the U(1) symmetry is the total number of particles in the universe. All processes need to respect this symmetry, and therefore need to have the same number of particles going in and coming out. In QCD, all quark flavors respect the symmetry separately and the number of quarks of each flavor is conserved. The electroweak sector mixes the flavors but the number of particles in general is still conserved.

In addition, there is an even larger, approximate symmetry. The masses of the lightest baryons and mesons are much larger than the masses of the two lightest quarks. The masses of the quarks shouldn't therefore make much of a difference to the spectrum of hadrons. We may first take these quarks to have approximately the same mass. Bundling them together in a vector

$$\Psi = \begin{pmatrix} \psi_u \\ \psi_d \end{pmatrix}$$

we can write the Lagrangian for the two lightest flavors as

$$\bar{\Psi}\left(i\gamma^\mu D_\mu - M\right)\Psi,$$

where M is the mass matrix

$$M = \begin{pmatrix} m_u & 0 \\ 0 & m_d \end{pmatrix} = \begin{pmatrix} m & 0 \\ 0 & m \end{pmatrix}. \tag{2.4}$$

D_μ is similarly a diagonal matrix of covariant derivatives.

In this form the Lagrangian is invariant under an SU(2) transformation

$$\bar{\Psi} \to \bar{\Psi} e^{-ic^a\sigma^a},$$
$$\Psi \to e^{ic^a\sigma^a}\Psi,$$

where σ^a are the generators of SU(2) and act on the indexes in the flavor vector we just introduced.

If this symmetry was exact protons and neutrons would have exactly the same mass. There is however a small difference in their masses, due to the difference in the masses of up and down quarks. Nevertheless we can see the effects of this approximate symmetry in the spectrum of hadrons and mesons.

The chiral symmetry is a bit more puzzling. This is the approximate symmetry that appears if we take the masses of the two lightest quarks to zero. This should be almost as good an approximation as taking the masses to be equal. The Lagrangian becomes

$$\bar{\Psi}\left(i\gamma^\mu D_\mu\right)\Psi.$$

In addition to the flavor symmetry above this is invariant under the transformation

$$\bar{\Psi} \to \bar{\Psi} e^{ic^a \sigma^a \gamma_5},$$
$$\Psi \to e^{ic^a \sigma^a \gamma_5} \Psi.$$

This is true since γ_5 anti-commutes with all γ_μ. If this was an exact symmetry, left- and right handed quarks would be completely decoupled. However we don't seem to observe this effect in nature. For example, if this symmetry held, pions and ρ mesons would have the same mass, but in nature pions are nearly massless and ρ mesons are massive. The explanation for this is that the chiral symmetry is spontaneously broken, the ground state of the system does not have the same symmetry as the Lagrangian. This is actually very similar to the spontaneous breaking the of electroweak symmetry by the Higgs particle.

In the case of QCD the breaking happens at such a large energy scale that it cannot be described by perturbation theory. We do observe the effects of the broken symmetry, however, in the spectrum of hadrons and mesons. It gives an expectation value to the chiral condensate

$$<\bar{q}q> \neq 0.$$

Since three symmetries are broken, there are three generators, there should be three massless Goldstone bosons. These are the pions, π^0, π^+ and π^-, and they are indeed very light compared to the other mesons. They are not exactly massless, though, since the symmetry is not exact.

2.3 The Electroweak Sector

The electroweak sector includes particles that are charged with respect to the electromagnetic and weak interactions, the gauge fields of these interactions and the Higgs boson. The Lagrangian is a bit more complicated since there are two interactions, but still quite simple.

$$L_{\mathrm{EW}} = L_{\mathrm{G}} + L_{\mathrm{F}} + L_{\mathrm{H}} \tag{2.5}$$
$$L_{\mathrm{G}} = -\frac{1}{4} B_{\mu\nu} B^{\mu\nu} - \frac{1}{4} W^a_{\mu\nu} W^{a\mu\nu} \tag{2.6}$$
$$L_{\mathrm{F}} = \sum_f \bar{\psi}_f \left(i\gamma^\mu D^f_\mu - m_f \right) \psi_f, \tag{2.7}$$
$$L_{\mathrm{H}} = |D_\mu h|^2 - \lambda \left(|h|^2 - v^2 \right)^2 \tag{2.8}$$
$$D^f_\mu = \partial_\mu - i g_f B_\mu - i g' W^a_\mu \lambda^a, \tag{2.9}$$
$$W^a_{\mu\nu} = \partial_\mu W^a_\nu - \partial_\nu W^a_\mu + g f^{abc} W^b W^c, \tag{2.10}$$
$$B_{\mu\nu} = \partial_\mu B_\nu - \partial_\nu B_\mu. \tag{2.11}$$

There are now two gauge bosons instead of the one in QCD. B_μ is the mediates the electromagnetic U(1) symmetry and W_μ the weak SU(2) symmetry. B_μ interacts with all quarks with different couplings g_f. The coupling to the SU(2) gauge boson W_μ is always the same, since it appears in the gauge part of the Lagrangian. The SU(2) interaction is actually not especially weak, but when the Higgs sector breaks the SU(2) symmetry, W_μ gets a large mass, which weakens the interaction.

The quarks coupling to W_μ are left-handed SU(2) doublets, with two colors. There are also right handed singlets that don't couple to W_μ. Now, when the symmetry is broken, both colors in the doublet become their own particles. This is why all the Standard Model fermions seem to come in pairs, electrons and μ- and τ-leptons have their neutrinos and

quarks have their own pairs, up and down, beauty and charm and top and bottom. This symmetric structure is actually born because the electroweak symmetry is broken.

The most important effect of the symmetry breaking is that the weak gauge bosons acquire a mass. The W^a_μ and B_μ bosons turn into the W^+_μ, W^-_μ and Z_μ and the photon A_μ. This allows us to describe weak interactions using a renormalizable quantum field theory. A model with massive gauge bosons is not renormalizable, but since at high energies the electroweak symmetry is not broken and the gauge bosons are massless, this is not a problem.

At the classical level, without including quantum mechanical effects, we can extract the zero temperature potential of the Higgs field from the Lagrangian,

$$V_\mathrm{H} = \lambda\left(|h|^2 - v^2\right)^2 \tag{2.12}$$

We see that the expectation value of the Higgs field is

$$|h|^2 = v^2.$$

The U(1) and SU(2) phases of the field remain undetermined. In fact, the model is symmetric with respect to the phases. Yet the field will have some phase, the Higgs field gets a phase randomly, and the vacuum is no longer symmetric. The symmetry in the Lagrangian is spontaneously broken.

So how does this affect the gauge bosons? To understand the theory when the symmetry is broken, we should expand the Lagrangian around the new vacuum. Let's write the Higgs doublet as

$$h = e^{i\theta(x)^a\lambda^a/2v}\begin{pmatrix} 0 \\ \chi{+}v \end{pmatrix}, \tag{2.13}$$

where χ is a field of real numbers with the expectation value 0. The angles θ^a give the SU(2) phases of the Higgs fields. There could also be a U(1) phase but it would just have the same effect as θ^0. The phases can be chosen any way we want by choosing the appropriate gauge and setting them to zero will simplify things:

$$\begin{aligned} &h \to e^{i\theta(x)^a\lambda^a/2v}h, \\ &\Rightarrow \theta^a = 0. \end{aligned}$$

By separating the χ and v parts Higgs part of the Lagrangian becomes

$$\begin{aligned} L_\mathrm{H} &= |D_\mu h|^2 - \lambda\left(|h|^2 - v^2\right)^2 \\ &= D_\mu\chi D^\mu\chi - 2\lambda v^2\chi^2 + \lambda v^4 \\ &+ \frac{v^2}{2}\left(g'W^{0\mu} - gB^\mu\right)\left(g'W^0{}_\mu - gB_\mu\right) \\ &+ \frac{v^2}{2}g'^2\left(W^{1\mu} - W^{2\mu}\right)\left(W^1{}_\mu - W^2{}_\mu\right). \end{aligned}$$

Reading from the above, χ is a boson with the mass $\sqrt{2\lambda}v$. Because we transformed θ^a away, we don't seem to have any Goldstone bosons, but the gauge bosons have gained masslike terms. To get this to the normal Standard Model form, let's redefine the gauge

fields.

$$\begin{aligned} W_\mu^+ &= W_\mu^1 + W_\mu^2, \\ W_\mu^+ &= W_\mu^1 - W_\mu^2, \\ Z_\mu &= \cos(\theta_W) W_\mu^0 - \sin(\theta_W) B_\mu, \\ \gamma_\mu &= \sin(\theta_W) W_\mu^0 - \cos(\theta_W) B_\mu, \\ \cos(\theta_W) = \frac{g'}{\sqrt{g^2+g'^2}}, &\quad \sin(\theta_W) = \frac{g}{\sqrt{g^2+g'^2}}. \end{aligned}$$

The two W bosons have the mass

$$v\frac{g}{\sqrt{2}}',$$

the Z boson has the mass

$$v\sqrt{\frac{g^2+g'^2}{2}}$$

and γ, the photon, is massless.

Now the weak gauge bosons appear to be massive. Thanks to the Higgs particle, we can also understand how the structure of weak interactions is generated from an SU(2) gauge theory. This means that all the interactions in the Standard Model are actually non-Abelian gauge theories, theories with a gauged local symmetry. Weak interactions are cast into the same model as electromagnetic and strong interactions, adding symmetry and elegance to the Standard Model.

There is just one more detail. Using the spontaneous symmetry breaking, we got rid of the gauge boson masses that would have caused the theory to fail at large energies. But fermions also have a mass, and adding them into the Lagrangian would break the SU(2) symmetry directly. Instead we can have the spontaneous symmetry breaking generate the fermion masses as well. Before the symmetry is broken fermions form left-handed SU(2) doublets and right-handed singlets. For example for up and down quarks we have

$$D = \begin{pmatrix} u_L \\ d_L \end{pmatrix}, u_R \text{ and } d_R.$$

Adding masses for u and d would couple them to the right-handed singlets and break the SU(2) symmetry. Instead we couple the fermions to the Higgs doublet,

$$L_{m_{u,d}} = h_u \bar{D} \cdot h_C u_R + h_d D \cdot h d_R.$$

h_C here is the charge conjugate of h. This is symmetric since we always take the product of two doublets and the U(1) charges add up to zero. When the electroweak symmetry is broken and h gets the expectation value 2.13, this becomes

$$(v-\chi)\left(h_u \bar{u}_L u_R + h_d \bar{d}_L d_R\right) = h_u v \bar{u}_L u_R + h_d v \bar{d}_L d_R + \ldots,$$

so that the up and down masses are $h_u v$ and $h_d v$.

This way we can explain also the fermion masses without needing to add them to the Lagrangian explicitly. Not all is perfect, however. The Higgs particle itself poses theoretical problems, although not nearly as severe as the ones it fixes. Since the Higgs particle is not a gauge boson but nevertheless couples to the fermions and the gauge bosons, its mass gets corrections in renormalization that grow as the renormalization scale squared. If at some large scale the Standard Model is replaced by some other, more fundamental model, that

would set the renormalization scale. The mass would need to be tuned just right to cancel the correction and produce the correct Higgs mass.

So if the scale of a grand unified theory, or GUT, is around $10^{16}GeV$, the correction to the mass would be around $10^{32}GeV$. Since the observed Higgs mass seems to be around $125GeV$, the right bare mass would have to be chosen extremely carefully. This is known as the fine-tuning or unnaturalness problem. The model just seems a bit contrived, not natural. This is at least one of the main reasons physicists expect there to be something beyond the Standard Model, that should show up at higher energies. Of course there are some purely empirical motivations as well, like dark energy and dark matter that the Standard Model does not incorporate.

2.4 Technicolor

Technicolor is one of the many models designed as a more natural replacement for the Higgs sector. Instead of adding the Higgs potential by hand and having it break a symmetry, technicolor uses a similar mechanism to the chiral symmetry breaking in QCD. The QCD chiral symmetry breaking actually already breaks the electroweak symmetry, the effect is just too small to explain the experimental data. In technicolor models there is a new strong interaction that breaks the electroweak symmetry at a larger scale, producing a bigger effect [4, 5, 6].

As it is, the chiral symmetry breaking only breaks the electroweak symmetry. It doesn't give masses to the fermions. To explain the fermion masses we have to extend the technicolor model to include four fermion interactions between the technicolor quarks and the Standard Model fermions [7, 8]. Adding these while staying within experimental bounds is only possible if the model belongs to a fairly restricted class of non-Abelian gauge theories, nearly conformal theories.

The simplest realization of a technicolor theory would be just a scaled version of QCD. It would have a chiral symmetry breaking around the electroweak scale, where the chiral condensate would acquire a non-zero expectation value

$$<\bar{t}_L t_R + \bar{t}_R t_L>\neq 0.$$

Here t is a technicolor quark. Since the left-handed quarks are SU(2) doublets and the right-handed ones are SU(2) singlets, this clearly breaks the electroweak symmetry. If the symmetry is exact and the Goldstone bosons truly massless, they can be absorbed to the gauge bosons, just as in the Higgs model.

When the fermions are massless the pions can be described by the effective chiral Lagrangian

$$\begin{aligned} L_\pi &= \frac{F_\pi^2}{4}\,\mathrm{Tr}\Big((D^\mu U)^\dagger (D_\mu U)\Big), \\ U &= e^{i\pi^a \lambda^a / F_\pi}. \end{aligned} \tag{2.14}$$

This is the same Lagrangian as in chiral perturbation theory for QCD, but in the case of technicolor, there are no correction from fermion masses. F_π is the pion decay constant, a parameter of the chiral effective action, and needs to be determined from experimental data or simulations. For QCD $F_\pi \approx 93MeV$.

The Lagrangian has a similar form to the Higgs Lagrangian in equation 2.8. The gauge boson masses come from the kinetic part of the Higgs Lagrangian. If we expand it in terms

of the phases θ, we have

$$|D_\mu h|^2 = \left|\partial_\mu \theta^0\right|^2 + \left|\partial_\mu \theta^1\right|^2 + \left|\partial_\mu \theta^2\right|^2 \tag{2.15}$$
$$+ v\left(\frac{g'}{2}W_\mu^0 + \frac{g}{2}B_\mu\right)\partial^\mu\theta^0 + \frac{g'}{2}vW_\mu^1\partial^\mu\theta^1 + \frac{g'}{2}vW_\mu^2\partial^\mu\theta^2 + \cdots .$$

This shows in a clear form that the phases θ^a are massless Goldstone bosons. The chiral Lagrangian in equation 2.14 can be expanded in the same way to get

$$\frac{F_\pi^2}{4}\mathrm{Tr}\Big((D^\mu U)^\dagger (D_\mu U)\Big) = \left|\partial_\mu \pi^0\right|^2 + \left|\partial_\mu \pi^1\right|^2 + \left|\partial_\mu \pi^2\right|^2 \tag{2.16}$$
$$+ F_\pi\left(\frac{g'}{2}W_\mu^0 + \frac{g}{2}B_\mu\right)\partial^\mu\pi^0 + \frac{g'}{2}F_\pi W_\mu^1\partial^\mu\pi^1 + \frac{g'}{2}F_\pi W_\mu^2\partial^\mu\pi^2 + \cdots .$$

It is easy to see from this from that that the Goldstone bosons behave in a similar way. When the chiral symmetry is broken, the weak symmetry is also broken, but instead of the Higgs expectation value v, the gauge boson mass is determined by the pion decay constant F_π.

The effect of the chiral symmetry breaking in QCD has on the gauge boson masses is

$$\delta M_W = \frac{1}{\sqrt{2}}gF_\pi \approx 29MeV,$$
$$\delta M_Z = \frac{1}{\sqrt{2}}\sqrt{g^2+g'^2}F_\pi = \frac{\delta M_W}{\cos(\theta_W)}.$$

Compared to the actual W mass this is so small that it can often be neglected. But if we scale the model so that the symmetry is broken at a larger energy scale, setting the pion decay constant to $246GeV$, we get the right masses for the weak gauge bosons. This simplest model is ruled out by precision electroweak observables, but similar models can be constructed by varying the number of colors and fermion flavors.

Just as with the Higgs symmetry breaking, the fermion masses combine a left-handed doublet to a right-handed singlet and break the electroweak symmetry. They should therefore be produced at the electroweak symmetry breaking. In extended technicolor fermions get their masses trough a coupling to the technicolor chiral condensate, which gets a nonzero expectation value when the chiral symmetry is broken.

The chiral condensate is a two fermion operator and the new mass terms include four fermions,

$$L_m = h_u \bar{D} u_R T \bar{t}_R,$$

where T and t_R are the new technicolor fermion doublet and singlet. A theory with four fermion interactions is not actually renormalizable, but it can be an effective description of a very high scale interaction, the extended technicolor or ETC interaction.

The ETC interaction could be a gauge force that couples to all the Standard Model fermions and technicolor fermions. In low energies this would couple technicolor fermions and Standard Model fermions to each other, but it would also, trough the same mechanism, couple them to themselves,

$$L_m = \alpha \bar{D} u_R D \bar{u}_R + \beta \bar{D} u_R T \bar{t}_R + \gamma \bar{T} t_R T \bar{t}_R. \tag{2.17}$$

The couplings α, β and γ should all be of the same order. If β now is large enough to produce the fermion masses, α should naively be just as large and produce visible flavor changing neutral currents. Since these are not observed, the naive version of extended technicolor doesn't seem to work. There is a way to correct this problem, but to find it we need to look at the dynamics of the technicolor model more carefully.

When the chiral condensate acquires and expectation value, the second term in equation 2.17 generates a mass for the Standard Model fermions. Since the interaction between the Standard Model fermion and the TC fermion is mediated by an ETC gauge boson, and the interaction happens at the ETC scale, we should also calculate the value of the chiral condensate at the ETC scale.

$$<\bar{t}t>_{\mathrm{ETC}} = \exp\left(\int_{\Lambda_{\mathrm{TC}}}^{\Lambda_{\mathrm{ETC}}} \frac{d\mu}{\mu}\gamma_m(\mu)\right) <\bar{t}t>_{\mathrm{TC}} \ . \tag{2.18}$$

Here γ_m is the mass anomalous dimension for technicolor fermion. It describes how mass-like quantities are renormalized when the scale changes. Λ_{ETC} and Λ_{TC} are the ETC and TC scales respectively.

If the difference between the scales is very large, or the mass anomalous dimension is large, the renormalization to the ETC scale can boost the fermion masses while the flavor changing neutral currents are not affected. For this to be the case, the coupling of the technicolor gauge theory should evolve very slowly with the energy scale. This would allow the integral over the anomalous dimension to accumulate considerably between the two scales.

In QCD the interaction evolves quite rapidly with the scale, but theories with different numbers of flavors or colors can behave very differently. The challenge is to find a model that evolves slowly enough and has an anomalous dimension large enough to produce the right masses for the Standard Model particles without creating too large flavor changing neutral currents.

2.5 Non-Abelian Gauge Theories

In QCD we have 3 colors and 6 quark flavors since that is what we see in particle accelerators. But there is nothing in the structure of the universe that compels us to use exactly 6 flavors and 3 colors. Actually the weak interaction seems to have 2 colors. We can expand these models to a larger group of quantum field theories, non-Abelian gauge theories. Originally these were a generalization of the U(1) electromagnetic model to non-Abelian SU(N) groups. Together with a varying number of fermion flavors, non-Abelian gauge theories exhibit a great variety of phenomenology and form the basis of the Standard Model.

The extension from U(1) to non-Abelian groups was actually formulated by Chen Ning Yang and Robert Mills already in 1954 [9], but since it couldn't include massive gauge bosons, like the weak gauge bosons W and Z, it wasn't initially successful. As the mechanism for giving gauge bosons mass through a spontaneous symmetry breaking was discovered in 1960, the models became more viable. The fundamental interactions in the Standard Model are gauge theories with a SU(3) and SU(2)×U(1) symmetries for QCD and the electroweak sector.

A general non-Abelian gauge theory coupled to a number of fermions is defined by the Lagrangian

$$L_{\mathrm{YM}} = -\frac{1}{4}\sum_{a=1}^{N_g} F^a_{\mu\nu}F^{a\mu\nu} + \sum_{f=1}^{N_f} \bar{\psi}_f \left(i\gamma^\mu D_\mu - m_f\right)\psi_f, \tag{2.19}$$

$$D_\mu = \partial_\mu - ig\sum_{a=1}^{N_g} A^a_\mu \Lambda^a, \tag{2.20}$$

$$F^a_{\mu\nu} = [D_\mu, D_\nu] = \partial_\mu A^a_\nu - \partial_\nu A^a_\mu + g f^{abc} A^b A^c. \tag{2.21}$$

Here N_g is the number of generators in the symmetry group. For SU(N), $N_g = N^2 - 1$. I

will often use the notation

$$A_\mu = \sum_{a=1}^{N_g} A_\mu^a \Lambda^a. \tag{2.22}$$

Generally speaking, the fermions interact with some representation of the symmetry group, and Λ^a are the generators of this representation. The gauge part of the action does not depend on the representation.

Depending on the symmetry group and the number and representation of the fermions, non-Abelian gauge theories can have very different dynamics. The electromagnetic and the strong interactions are both examples of gauge theories coupled to fermions. Nevertheless they do share some important characteristics. They all have the chiral and flavor symmetries discussed in the previous chapter, at least if the quarks have a small mass. The chiral symmetry is not always broken, however, and the parameter range where the breaking happens is still being mapped. Some of the models are confining, like QCD, and some have free quarks, like QED.

The parameters in 2.19 are not actually physically measurable. The values for the coupling g and the mass m need to be renormalized to get the measured values and quantum corrections affect them. In both QCD and QED the coupling depends on the energy scale of the process it is measured from, for example the energy of two colliding particles. In QED it increases with energy and in QCD it decreases with energy.

Since the coupling runs to different directions in these two theories, we can imagine that there could be a model, structured like QCD and QED, where the coupling actually stays constant. A model like this would be called conformal and it would be completely independent of the energy scale. In order to build a working technicolor theory we actually need a non-Abelian gauge model that changes slowly with the scale, a nearly conformal model. This would be a model just outside the parameter range for conformal theories but on the other hand in the right parameter range for a chiral symmetry breaking.

The free parameters of the model are the interaction strength, codified by g, and the fermion masses. Since a nonzero fermion mass would add an energy scale to the model, so that it could not be scale independent, we should confine ourselves to models with zero fermion masses. This seems like a sensible assumption since in the Standard Model all masses are created when the electroweak symmetry is broken.

In a massless theory the only parameter that changes with the energy scale μ is the renormalized coupling constant g. It's scale dependence is described by the β-function, defined as

$$\beta(g) = -\mu \frac{dg}{d\mu}, \tag{2.23}$$

where μ is the energy scale of the process being described. The value of the β function has been worked out to four-loop order in perturbation theory for a general gauge theory [18]. The first two terms in the perturbative expansion are given by

$$\beta(g) = -\frac{\beta_0}{16\pi^2} g^3 - \frac{\beta_1}{16\pi^2)^3} g^5, \tag{2.24}$$

$$\beta_0 = \frac{11}{3} N - \frac{4}{3} T(R) N_f, \tag{2.25}$$

$$\beta_1 = \frac{34}{3} N^2 - \frac{20}{3} T(R) N_f - 4 C_2(R) T(R) N_f, \tag{2.26}$$

where $T(R)$ and $C_2(R)$ are the group theory factor and the quadratic Casimir coefficient for the representation of the gauge group that fermions transform in. For example for the

fundamental representation of SU(N) $T(R) = T(F) = 1/2$ and $C_2(R) = C_2(F) = (N^2 - 1)/(2N)$ and for the adjoint representation $T(A) = N$ and $C_2(A) = N$.

In a truly conformal model the value of the β-function would be zero everywhere. It seems that such a non-Abelian gauge theory does not exist, either the first of the second term in 2.24 is non-zero. However it is possible to find a model with a nontrivial infrared fixed point, a value of the coupling $g = g^*$ where the β-function is zero. In a model like this the coupling would run to the fixed point at low energies and then stay virtually constant.

From equation 2.24 we can find a first order guess for a fixed point, where the value of the β-function is zero,

$$g^{*2} = -16\pi^2 \frac{\beta_0}{\beta_1}.$$

When β_0 is negative, the beta-function starts positive at small coupling and the model doesn't have asymptotic freedom. This gives a maximum number of fermions for a model with a conformal fixed point,

$$\begin{aligned} \beta_0 = 0 &= \frac{11}{3}N - \frac{4}{3}T(R)N_f \\ \Rightarrow N_f &= \frac{11}{4}N/T(R). \end{aligned}$$

For a model with fermions in the fundamental representation the upper limit increases with the number of colors. With adjoint fermions the limit is constant, $N_f \leq 2$.

The upper limit in fermion flavors is described well by perturbation theory, since the fixed point moves towards $g^* = 0$. Above it the β-function starts positive and the coupling runs to higher values with the energy scale. This means that there is no confinement and no chiral symmetry breaking. Models over the upper limit cannot be used as technicolor theories. We wish to find a model near the lower limit in the number of fermion flavors, where the β function is negative and the coupling runs to zero as the energy increases. These theories can be confining and can have a chiral symmetry breaking. Unfortunately the lower limit is much harder to identify, since the fixed point moves to larger couplings when the number of fermions decreases.

One can of course use perturbation theory to calculate an approximation for the lower limit. When the chiral symmetry is broken, the chiral condensate gets an expectation value and creates mass-like scale for the model. This means that it cannot be scale invariant anymore, and so cannot have a fixed point. An estimate for the critical coupling where this happens can be calculated by building an effective action for the chiral condensate [10] and minimizing it. The first order estimate for the critical coupling where the chiral symmetry is broken is at

$$g_c^2 = \frac{4\pi^2}{3C_2(R)}.$$

When the fixed point crosses the critical coupling the model is no longer conformal [11]. This happens at

$$\begin{aligned} g^* &= g_c \\ \Rightarrow \beta_0 &= \frac{\beta_1}{12C_2(R)} \end{aligned}$$

This also gives an ascending line for a model with fundamental fermions and a constant for a model with adjoint fermions.

Putting the lower and the upper limit together, we find that there is a conformal window in the parameter space, an area where the non-Abelian gauge models have a nontrivial infrared

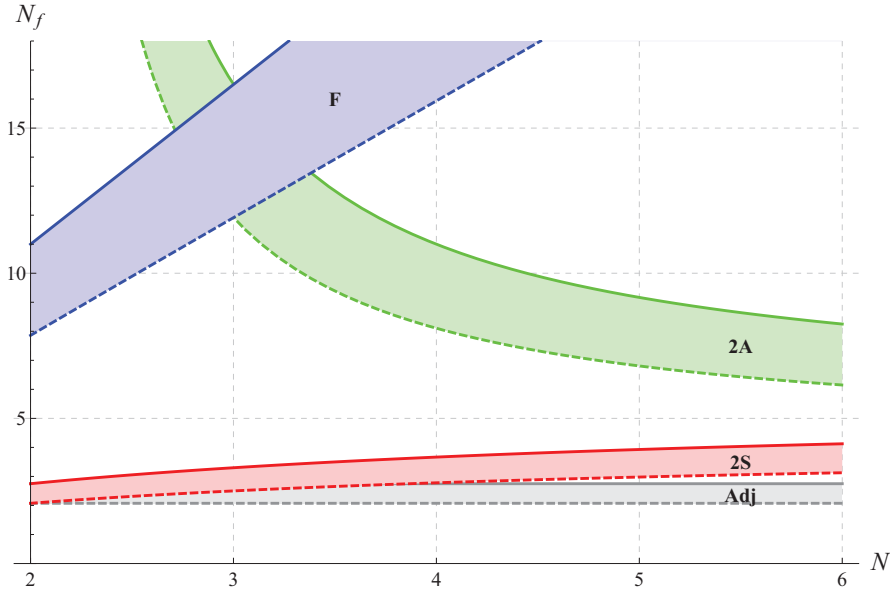

Figure 2.2: The conformal window in colors and fermion flavors. The fundamental representation is labeled by F, the adjoint by Adj, the two-index symmetric by 2S and the two-index anti-symmetric by 2A.

fixed point. In figure 2.2 we show the upper and the lower limit for the conformal window in terms of colors and fermion flavors for SU(N) with fermions in the fundamental, adjoint, two-index symmetric and two-index anti-symmetric representations.

The critical coupling for the chiral symmetry breaking tends to have a high value, so high that perturbation theory no longer works. The chiral symmetry breaking itself is a non-perturbative effect. The estimate for the lower limit is therefore only a guess and finding the actual value requires some methods other than the perturbative expansion. Nevertheless we do wish to find a theory below the lower limit, but close to it, and see whether it exhibits a chiral symmetry breaking.

To study the models in the non-perturbative region, we turn to lattice field theory. We simulate the full dynamics of the model from first principles and measure the behavior of the coupling with respect to the energy scale to find whether the theory has a conformal fixed point of not.

Chapter 3

Lattice Simulations

3.1 Fields on the lattice

Quantum field theories describe the behavior of fields that are continuous, like the height of the oceans surface or the density of air. There are no separate particles as such, but waves in these fields. In principle they can only be completely described by an infinite amount of numbers, there is an infinite amount of points even in a finite volume. When simulating the theory we of course can have only a finite number of points, and the system is usually divided into a lattice, as in figure 3.1, in the hope that if one makes the distance between the points small enough, the difference between the lattice and the real continuum theory is small.

The dynamics of a quantum field theory are calculated from its action S, the sum of its Lagrangian at all points in space and time. The probability to find the field in a certain configuration Ψ_1 at a time t_1 is given by

$$P_{\Psi_1} = \left| \frac{\int_{\Psi(t_1)=\Psi_1} d\Psi e^{-iS(\Psi)}}{\int d\Psi e^{-iS(\Psi)}} \right|^2 . \tag{3.1}$$

This is the path integral formulation of quantum mechanics. The integral in the numerator sums over all the possible configurations of fields, where at time t_1 the fields are in the state Ψ_1. In the denominator we just sum over all possibilities whatsoever, so that the probability that something happens is 1. The importance, or weight, of a certain configuration is then given by the $\exp(-iS)$ part. Things are a little more complicated than they seem, though.

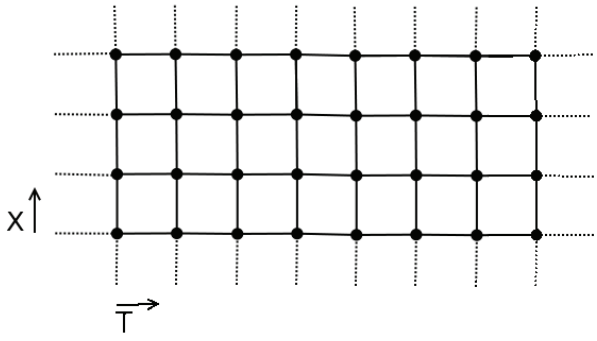

Figure 3.1: The fields are divided on a lattice. The fermion fields $\phi(x)$ exist on the nodes and the gauge fields $U(x, a\hat{\mu})$, that describe the interaction, on the links between the nodes.

The size of the weight is always one and it can be negative or even imaginary, so that the configurations can cancel each other out. One really would need to sum over all possible configurations to know the result and the possibilities are infinite.

The lattice simulation approach tackles these problems by creating an approximate effective model, which parallels the physical situation but is less complicated mathematically. We can start from the general action of a non-Abelian gauge theory with fermions,

$$S = \int d^3x dt \left[-\frac{1}{4} \mathrm{Tr}\big(F^a_{\mu\nu} F^{a\,\mu\nu}\big) + \bar{\phi}\,(i\gamma^\mu D_\mu - m)\,\phi \right]. \tag{3.2}$$

The usual trick is to let the time evolve to the imaginary direction, in other words to do the transformation $t \to i\tau$. The integral over time then transforms as $dt \to id\tau$. This also means that the space-time becomes Euclidean, the metric tensor becomes just the identity matrix. We can now write an Euclidean version of the action as

$$S_\mathrm{E} = -iS(t \to i\tau) \tag{3.3}$$

$$= \int d^3x d\tau \left[\frac{1}{2} \mathrm{Tr}({}^a F_{\mu\nu} F^{a\,\mu\nu}) + \bar{\phi}\,(i\gamma^\mu D_\mu + m)\,\phi \right]. \tag{3.4}$$

And now probability from the path integral is

$$P_{\Psi_1} = \left| \frac{\int_{\Psi(t_1)=\Psi_1} d\Psi e^{-S_\mathrm{E}(\Psi)}}{\int d\Psi e^{-S_\mathrm{E}(\Psi)}} \right|^2. \tag{3.5}$$

The time evolution (in τ) of this new model does not correspond to the time evolution (in t) of the physical system, but many physical observables can still be calculated from it. The weight $\exp(-S_\mathrm{E})$ from the path integral is now number that is larger than zero and the configurations where it's small are not as important in the integral as the ones where it's large. All the configurations are not needed to calculate this integral to a good accuracy, just the ones where S_E is small and $\exp(-S_\mathrm{E})$ is large. We will use the Euclidean action from now on and drop the label E.

The gauge field A_μ is really a part of the generalized covariant derivative D_μ. It describes how a fermion field at a certain point changes when freely moving to another point. This is called parallel transporting the vector, a term coming from geometry and gravitation. The field $\phi(x)$ as seen from the point $x - a\hat{\mu}$, were $\hat{\mu}$ unit vector to direction μ and a is the distance, is

$$U(x, a\hat{\mu})\phi(x) = e^{\int_x^{x+a\hat{\mu}} dx\, iA_\mu(x)} \phi(x). \tag{3.6}$$

On the lattice we use the matrix U to describe the gauge field. It is a matrix that belongs to the group of special unitary $N_c \times N_c$ matrices, $\mathrm{SU}(N_c)$. If we divide the world to a lattice where the distance between the closest points is a, the whole gauge field is described by the set of matrices $U_\mu(x) = U(x, a\hat{\mu})$, for all the space-time points x on the lattice. Writing out the definition of A_μ in equation 2.22, we see that the field $U_\mu(x)$ can be written in terms of the generators of the group,

$$U_\mu(x) = e^{U^a_\mu(x)\Lambda^a}. \tag{3.7}$$

The fermion fields are Grassman numbers and we cannot do operations directly with them on a computer. Instead we can formally integrate over the fermion fields in the path integral,

$$Z = \int_\phi d\phi d\bar{\phi}\, e^{-\int d^4x \bar{\phi}(x)(i\gamma^\mu D_\mu - m)\phi(x)} = \int_\phi d\phi d\bar{\phi} e^{-\int d^4x \int d^4y \bar{\phi}(x) M(x,y) \phi(y)}$$

$$= \det_{x,y}(M(x,y)).$$

The determinant of M is just as hard to evaluate as the integral itself, but the Grassman fields have disappeared. To evaluate the determinant we can write it as an integral of a field of complex numbers ψ and $\bar{\psi}$,

$$Z = \det_{x,y}(M(x,y)) = \int_{\psi} d\psi d\bar{\psi} e^{-\int d^4x \int d^4y \bar{\psi}(x) M^{-1}(x,y) \psi(y)}. \tag{3.8}$$

The fermion field on the lattice is now described by vectors ψ and $\bar{\psi}$ of N_C complex elements.

3.2 Discretized action

After making the fields discrete, the action itself must be written in a discrete form. When we take the continuum limit, meaning that $a \to 0$ while the physical size of the system remains the same, this discretized action should approach the original one. There are many ways to do this and naively one would expect them to be equally valid. Unfortunately some problems emerge when discretizing the fermion action and one must take some care in choosing it.

The field strength tensor $F^{\mu\nu}$ in the gauge action essentially describes the change in a vector when parallel transported around a small loop. In the discretized version we use a plaquette $U_{\mu\nu}$, a parallel transport around the smallest squares on the lattice. The gauge part is usually discretized as

$$\begin{aligned}
&- \int d^4x \frac{1}{2} F^a_{\mu\nu} F^{a\,\mu\nu} = \sum_{x,\mu>\nu} \beta \left[1 - \frac{1}{N} \mathrm{ReTr}(U_{\mu\nu}(x)) \right], \\
&U_{\mu\nu}(x) \\
&= U(x, a\hat{\mu}) U(x + a\hat{\mu}, a\hat{\nu}) U(x + a\hat{\mu} + a\hat{\nu}, -a\hat{\mu}) U(x + a\hat{\nu}, -a\hat{\nu}) \\
&= U_\mu(x) U_\nu(x + a\hat{\mu}) U^\dagger_\mu(x + a\hat{\nu}) U^\dagger_\nu(x), \\
&\beta = \frac{2N}{g^2}
\end{aligned} \tag{3.9}$$

Notice that here

$$U(x, -a\hat{\mu}) = U^\dagger(x - a\hat{\mu}, a\hat{\mu}).$$

If we expand the lattice action around $a \to 0$, we see that it approaches the original continuum action.

The fermion part of the action is a little more complicated. We can start by doing it the obvious way, replacing the covariant derivative with a parallel transported discrete derivative:

$$S_F = \sum_{x,y} \bar{\phi}(x) \left(\not{D}_{xy} + m\delta_{xy} \right) \phi(y), \tag{3.10}$$

$$\not{D}_{xy} = \frac{1}{2} \gamma^\mu (\Delta_{\mu,xy} - \Delta^*_{\mu,xy}), \tag{3.11}$$

$$\Delta_{\mu,xy} = \frac{1}{a} \left(U_\mu(x) \delta_{x,y-a\hat{\mu}} - \delta_{xy} \right), \tag{3.12}$$

$$\Delta^*_{\mu,xy} = \frac{1}{a} \left(\delta_{xy} - U^\dagger_\mu(x - a\hat{\mu}) \delta_{x,y+a\hat{\mu}} \right), \tag{3.13}$$

where ϕ is again a Grassman field. If we add together the derivative parts and simplify we have

$$\not{D}_{xy} = \frac{1}{2a} \sum_\mu \gamma^\mu \left(U_\mu(x) \delta_{x,y-a\hat{\mu}} - U^\dagger_\mu(x - a\hat{\mu}) \delta_{x,y+a\hat{\mu}} \right) \tag{3.14}$$

This is often called the naive fermion action and it does seem to be the simplest discrete representation of the fermion action. Unfortunately, it does not reproduce the original action in the continuum.

We can see the problem by considering the non-interacting case, where all the gauge fields U are unity. Then the Naive action reads

$$S_F = \sum_{x,y} \bar{\phi}(x) \left[m\phi(x) + \frac{i}{2a} \sum_{\mu} \gamma^{\mu} (\phi(x + a\hat{\mu}) - \phi(x - a\hat{\mu})) \right]. \tag{3.15}$$

In one dimension, every periodic field $\phi(x)$ can be presented as a Fourier series

$$\phi(x) = \sum_{n} c_n \exp\left(i \frac{2\pi n}{L} x \right),$$

where L is the length of the lattice. Since the lattice is discrete, it suffices to include the terms where $n < L/a$. This is referred to as the Brillouin zone. Since all that matters is the value of $\phi(x)$ at the lattice points $x = ma$, the terms at the lower and the upper end of this zone are identical, $\exp(0) = \exp(i2\pi m)$. Both modes of ϕ behave like zeros of the derivative, and describe physical particles. So the discrete fermion field $\phi(x)$ actually describes two fermion fields in continuum. The extra fields are called doublers and in four dimension there are 15 of them.

There are several ways to remedy this problem and all of them lose something from the original theory. The original proposal by Wilson eliminates the doublers by adding a term to the fermion action that doesn't affect the normal fermion, but gives the doublers an infinite mass in the continuum limit. The added term directly breaks the chiral symmetry. Another very popular approach, staggered fermions, uses some of the doublers to construct Dirac components to the fermions, leaving only four doubler at the cost of flavor symmetry and a part of the chiral symmetry. Then one either just simulates with four fermions or removes some of them by adding a fourth root to the action. There is also a way to eliminate the doublers and keep the chiral symmetry exactly, domain wall fermions, but these introduce an extra fifth dimension and are therefore very expensive to simulate.

We will consider Wilson fermions here. The term added to the action resembles a second derivative. We can write out the Wilson-Dirac operator as

$$\begin{aligned} \not{D}_{xy} &= \frac{1}{2}\gamma^{\mu}(\Delta_{\mu,xy} - \Delta^{*}_{\mu,xy} - \frac{a}{2}\Delta_{\mu,xz}\Delta_{\mu,zy}), \\ &= \frac{1}{2a} \sum_{\mu} \left((\gamma^{\mu} - 1) U(x, a\hat{\mu}) \delta_{x,y-a\hat{\mu}} - (\gamma^{\mu} + 1) U^{\dagger}(x - a\hat{\mu}, a\hat{\mu}) \delta_{x,y+a\hat{\mu}} + \frac{4}{a}\delta_{xy} \right) \end{aligned}$$

If we include the fermion mass we get what is called the fermion matrix

$$\begin{aligned} M_{xy} &= \not{D}_{xy} + m\delta_{xy} \\ &= \frac{1}{2a} \sum_{\mu} \left((\gamma^{\mu} - 1) U(x, a\hat{\mu}) \delta_{x,y-a\hat{\mu}} - (\gamma^{\mu} + 1) U^{\dagger}(x - a\hat{\mu}, a\hat{\mu}) \delta_{x,y+a\hat{\mu}} \right) \\ &+ \left(\frac{4}{a} + m \right) \delta_{xy}. \end{aligned}$$

Finally, we can simplify this by normalizing the fermion field and get

$$\begin{aligned} M_{xy} &= \delta_{xy} \\ &+ \kappa \sum_{\mu} \left((\gamma^{\mu} - 1) U(x, a\hat{\mu}) \delta_{x,y-a\hat{\mu}} - (\gamma^{\mu} + 1) U^{\dagger}(x - a\hat{\mu}, a\hat{\mu}) \delta_{x,y+a\hat{\mu}} \right), \\ \kappa &= \frac{1}{8 + 2ma}. \end{aligned}$$

The parameter κ is called the hopping parameter, since it describes the coupling between fermions at different points on the lattice.

As we can see, there is now a term in the action that resembles a mass term, even if the fermion is actually completely massless. This means that the chiral symmetry remains explicitly broken even at zero mass. Adding the extra term also introduces errors of order a to the measurements. The naive fermion action was accurate to order a^2, except for the fact that it included doublers. The term we added, however, carries an explicit factor of a. It disappears in continuum, but more slowly than the error in the naive action.

The fermion fields here are still Grassman numbers and in the simulations we need to use complex numbers. After the trick in equation 3.8 the fermion action becomes

$$S_F = \sum_{x,y} \bar{\psi}(x) M_{xy}^{-1} \psi(y). \tag{3.16}$$

ψ is a field of complex vectors with N_c color degrees of freedom and 4 Dirac degrees of freedom. This is finally a form that can be used in lattice simulations. The fermion matrix has to be inverted every time the action is calculated and this is actually the most time consuming part in simulations with modern algorithms.

Generating fermion configurations becomes significantly easier if we make the fermion term Gaussian. The fermion matrix is not necessarily positive definite, but we can combine two degenerate flavors of fermions in the action to get a positive matrix,

$$Z_F = e^{\sum_{x,y} \bar{\psi}_1(x) M_{xy}^{-1} \psi_1(y) + \sum_{x,y} \bar{\psi}_2(x) M_{xy}^{-1} \psi_2(y)} \tag{3.17}$$

$$= \det(M)^2 = \det(M^2) = e^{\sum_{x,y} \bar{\psi}(x) M_{xy}^{-2} \psi(y)}. \tag{3.18}$$

This version restricts us to use an even number of flavors but using approximations like the rational hybrid Montecarlo it is also possible to simulate with an odd number of fermions.

Gathering together the gauge and fermion parts we can write down the entire lattice action. We will write it in lattice units, which means that all values are scaled with an appropriate power of a to make them dimensionless and a is then put to 1. This is the form used in simulations, since in numerical work everything needs to be dimensionless. In lattice units the action is

$$S = \sum_{x,y} \left[\sum_{\mu>\nu} \beta \left[1 - \frac{1}{N} \mathrm{ReTr}(U_{\mu\nu}(x)) \right] + \bar{\psi}(x) M_{x,y}^{-2} \psi(y) \right], \tag{3.19}$$

$$M_{xy} = \delta_{xy} + \kappa \not{D}_{xy}, \tag{3.20}$$

$$\not{D}_{xy} = \sum_{\mu} \left((1-\gamma^\mu) U(x,\hat{\mu}) \delta_{x,y-\hat{\mu}} + (1+\gamma^\mu) U^\dagger(x-\hat{\mu},\hat{\mu}) \delta_{x,y+\hat{\mu}} \right) \tag{3.21}$$

3.3 Generating Configurations

Now that theory is discretized and we have a consistent action, we need to generate configurations of fields from the correct distribution. This is at the heart of a lattice simulation program. Basically the most straightforward way do generate the configurations would be to draw random numbers for all the fields and calculate the measurements with the weight in 3.1. For most of the possible configurations the action would be very large and the weight extremely small so that we would end up doing an enormous amount of extra work. Fortunately there are ways to generate just the relevant configurations.

It's fairly simple to generate random configurations of the fermion fields. Given a configuration of gauge fields we can write the distribution of the fermion fields as

$$Z_\psi = \int d\psi e^{-\sum_{x,y}\bar{\psi}(x)M^{-2}_{xy}\psi(y)} = \int d\psi e^{-\sum_x \bar{\chi}(x)\chi(x)},$$
$$\chi(x) = \sum_y M^{-1}_{xy}\psi(y).$$

The field χ has a Gaussian distribution. To generate a fermion configuration, one generates a Gaussian field χ and then calculates ψ.

Unfortunately the gauge part of the action is not Gaussian and we cannot just draw random numbers to fill it. Instead the configurations are generated using a Markov chain. Starting from some more or less relevant configuration, one introduces random changes to the gauge matrices. Each change needs to fulfill 3 criteria to to produce the correct distribution of configurations. The first two are natural, it has to be possible to go from any one state to any other in a finite number of steps and the propabitility of generating some configuration has to be one. Here I denote any two states as i and i' and the propability for going form i to i' in a n steps as $P_n(i \to i')$. For just one step I use $P_1(i \to i') = P(i \to i')$. The first condition translates into

$$\forall i, i', P_n(i \to i') > 0 with some n \in \mathcal{N}, \tag{3.22}$$

and the second condition into

$$\sum_{i'} P(i \to i') = 1. \tag{3.23}$$

The third condition is known as the balance equation,

$$\sum_{i'} P(i \to i')e^{-S(i)} = \sum_{i'} P(i' \to i)e^{-S(i')}, \tag{3.24}$$

that is, the sum of the probabilities of all possible endpoints weighed by the desired probability is the same as the sum of the probabilities of coming back weighed by the probability of the endpoint. This ensures that we eventually end up with a correctly distributed set of states. Using eq. 3.23 we can write it in the form

$$\sum_{i} P(i \to i')e^{-S(i)} = e^{-S(i')}. \tag{3.25}$$

So the desired distribution, $\exp(-S(i))$, is a fixed point of the update process. If we update a correctly distributed set of configurations, the distribution will not change. Since we sample trough the entire configuration space in a finite time, no matter the starting distribution, we should in the end have the correct distribution.

In practice the simulation algorithms are designed to fulfill a more restricted form of the balance equation, the detailed balance equation,

$$P(i' \to i)e^{-S(i')} = P(i \to i')e^{-S(i')}. \tag{3.26}$$

Here the balance equation holds for each possible new configuration separately. This requirement is more restrictive but if it holds, the balance equation certainly holds, and it is easier to conceptualize.

Next we need a method for generating the next configuration from the previous one that fulfills all the given requirements. One of the simplest possibilities would be the Metropolis

algorithm. Starting from some configuration we randomly propose a new one and accept it at a certain probability. If the probability of the proposing i' is $Q(i, i')$, the acceptance probability should be

$$P(i \to i') = \max(1, \frac{e^{-S(i')}Q(i', i)}{e^{-S(i)}Q(i, i')}).$$

The proposal probability has to be either symmetric, $Q(i', i) = Q(i, i')$, or independent of the origal distribution. In both cases the update fulfills all the properties above and samples just the important configurations. It works very well when the action is local, there are interaction only between neighboring points. Then we can change just one point at a time on calculate the change in the action quickly. Unfortunately the fermion part of the action is not local, since we have to calculate the inverse of the fermion matrix. Changing just one matrix on the lattice will affect the action at all points.

The Hybrid algorithm is designed to update the entire configuration at once. To do this we first need to add and extra field to the model. We can always multiply the distribution with a constant, such as an integral over a new conjugate field $\Omega(x, \mu)$,

$$\begin{aligned} Z(U, \psi, \Omega) &= Z(U, \psi) \int d\Omega e^{-\sum_{x,\mu} \frac{1}{2}\mathrm{Tr}\,(\Omega(x,\mu)\Omega(x,\mu))} \\ &= \int d\Omega dU d\psi e^{-\sum_x \left[\mathcal{L}_\psi + \mathcal{L}_U(x) + \sum_\mu \frac{1}{2}\mathrm{Tr}\,(\Omega(x,\mu)\Omega(x,\mu))\right]}. \end{aligned}$$

Naturally any expectation values measured using this new action will be the same as the ones using the old ones. The things we want to measure will not even depend on the new field. The distribution of the new field is Gaussian, so that it's simple to generate random configurations of it.

To generate new gauge configurations we generate this conjugate field Ω and let the system evolve along the classical equations of motion. Ω basically functions as the momentum of the gauge field. As we see from equation 3.7, there are as many degrees of freedom in the gauge fields as there are generators in the group that the gauge matrices U belong to. If we add a momentum Ω^a for each of the generators a, we can write them as a sum of the generators, a traceless antihermitean matrix

$$\Omega = \omega^a \lambda^a$$

Since the action is conserved in classical mechanics, we should end up with a new configuration that has the same action as the previous one. The action does change when we generate new fields for fermions and the conjugate fields, so that all possible configurations are covered. This can be repeated to generate a chain of configurations.

The classical equations of motion are

$$\frac{d\omega^a(x, \mu)}{dt} = \frac{dS}{dU(x, \mu)} \frac{dU(x, \mu)}{dU^a(x, \mu)}$$

and

$$\frac{dU^a(x, \mu)}{dt} = d\omega^a(x, \mu).$$

These of course need to be integrated numerically. One of the simplest methods for doing the integration is the leapfrog integrator. We evolve the configuration G in small discrete steps given by

$$\begin{aligned} G(t + \Delta t) &= U_G(\Delta t/2) F(\Delta t) U_G(\Delta t/2) G(t), \\ U_G(\Delta t) G &= \left[\forall a, x, \mu,\, U^a_\mu(x) \to U^a_\mu(x) + \Delta t\, \omega^a_\mu(x)\right], \\ F(\Delta t) G &= \left[\forall a, x, \mu,\, \omega^a_\mu(x) \to \omega^a_\mu(x) + \Delta t \frac{dS}{dU^a_\mu(x)}\right], \end{aligned}$$

where Δt is the step in simulation time. The gauge field is first updated only half way and the momentum field leaps over it and is updated a full step. Then the gauge field catches up and is updated the other half step.

After generating a fermion and a momentum configuration one integrates over a certain amount of time steps, a trajectory. The step size Δt and the length of the trajectory are tunable parameters. In the end one has, up to errors in the numerical integration, a new gauge configuration in the Markov chain. Of course if one used just the Hybrid method, the errors in the numerical integration would have to be very small.

The most used method for generating configurations, the Hybrid Montecarlo or HMC, is a combination of the Hybrid- and the Metropolis methods. We can consider the new gauge configuration generated by the Hybrid method trajectory as a proposal in the Metropolis method. We calculate the change in the action and approve the new configuration at the probability

$$P(i \to i') = \max(1, e^{-S(i')+S(i)}).$$

If the new configuration is not accepted, we just use the old one. All measurements should of course be done after every update, whether or not the new gauge configuration was accepted.

So far HMC is the most efficient method for generating gauge configurations. It can be tweaked a bit by improving the integrator or dividing the fermion fields differently. Examples of the second are the rational hybrid Montecarlo [15] that allows one to simulate with an odd number of fermions and the Hasenbusch method [16] where the fermion field is divided into a low and a high mass part. Generally the most expensive part of the simulation is updating the momentum field, where one has to take the derivative of the fermion part of the action.

3.4 Improving the Algorithm

Since we want to probe the behavior of the lattice models at very strong coupling, where the interaction between points are strong and the simulations tend to be heavy, improvements in the simulation algorithms are welcome. A reduction in computation time allows for longer simulations and greater statistical accuracy, or simulations on more values of the bare coupling and reduced systematic uncertainty. Most algorithmic improvements do not reduce the simulation time enough to allow using larger lattice sizes, but they do bring that possibility closer as well.

The most obvious starting place is the integrator, the algorithm for evolving the gauge configuration along the classical equations of motion in the HMC algorithm. Most of the simulation time is spent in calculating the inverse of the fermion matrix, which is required for the fermion part of the momentum step.

We can divide the force, the derivative of the momentum, into a gauge part and the fermion part,

$$\begin{aligned} F_\mu(x) &= F_{\mu,U}(x) + F_{\mu,F}(x), \\ F_{\mu,U}(x) &= \frac{dS_U}{dU^a_\mu(x)}, \\ F_{\mu,F}(x) &= \frac{dS_F}{dU^a_\mu(x)}. \end{aligned}$$

Compared to the fermion part, the gauge part is rather cheap to evaluate. Especially at weaker couplings the gauge part is also larger than the fermion part and is responsible for a larger part of the integration error. The fermion part doesn't actually need to be updated as often as the gauge part.

A multiple time scale integrator could be something like a generalized leapfrog step, where the gauge field and the gauge part of the force are updated more often than the fermion part of the force. We can use the notation

$$F_G(\Delta t) = \left[\forall a, x, \mu,\, \omega^a_\mu(x) \to \omega^a_\mu(x) + \Delta t \frac{dS_G}{dU^a_\mu(x)}\right],$$
$$F_F(\Delta t) = \left[\forall a, x, \mu,\, \omega^a_\mu(x) \to \omega^a_\mu(x) + \Delta t \frac{dS_F}{dU^a_\mu(x)}\right]$$

for the gauge and the fermion parts of the force respectively. One possible multiple time scale leapfrog step could be

$$G(t+\Delta t) = U_G(\frac{\Delta t}{4})F_G(\frac{\Delta t}{2})U_G(\frac{\Delta t}{4})F_F(\Delta t)U_G(\frac{\Delta t}{4})F_G(\frac{\Delta t}{2})U_G(\frac{\Delta t}{4})G(t)$$

Shortening the time step for the gauge part reduces the integration error and allows increasing the step size. Since we haven't added any fermions steps, the computation time is almost the same. Unfortunately this only works well if the gauge force is at least as large as the fermion force, which is sometimes not true when the coupling is large.

Of course the leapfrog integrator is the just the simplest possibility and probably not the most effective. It is the only possible first order integrator with just one force step. If we allow a second fermion force update, there is a bit more freedom. Taking into account that the integration should be symmetric in time, the general second order integrator is

$$G(t+\Delta t) = U_G(\zeta\Delta t)F(\frac{\Delta t}{2})U_G([1-2\zeta]\Delta t)F(\frac{\Delta t}{2})U_G(\zeta\Delta t)G(t),$$

where F is a general force step.

Assuming that the two operations have about the same magnitude, the optimal value for ζ is roughly 0.2 [12, 13]. The error of one of these Omelyan integrator steps is about 30% of the error of a leapfrog step. This means that the step size can be more than doubled, but the computation time is only doubled. Using the Omelyan integrator we have reduced the computation time by about 50%. We have combined this with a multiple step size integrator for a little further improvement.

Another good part of the algorithm to improve is the inversion of the fermion matrix. For every fermion force step one needs to solve the equation

$$Mx = \psi. \tag{3.27}$$

This is usually done using the conjugate gradient algorithm. The algorithm starts from some initial guess and first takes the negative gradient of the guess with respect to the matrix. Then it builds a basis of vectors that are conjugate to the gradient, hence the name, by taking the part of the residual $Mx - \psi$ that is conjugate to all the previous vectors.

If the initial guess is closer to the solution the algorithm naturally finds it faster, so it's useful to find as good an initial guess as possible. Since the gauge field is changed only a small amount between force calculations, the previous solutions should be close to the next one. The chronological initial guess [14] is constructed by solving equation 3.27 in the space of a few earlier solutions. If the solutions from n previous time steps were ψ_n, the basis

vectors are

$$\begin{aligned} v_1 &= \frac{\psi_1}{|\psi_1|}, \\ v_2 &= \frac{v_2'}{|v_2'|},\ v_2' = \psi_2 - \frac{v_1 \cdot \psi_2}{|v_1|^2} v_1, \\ &\dots \\ v_n &= \frac{v_n'}{|v_n'|},\ v_n' = \psi_n - \sum_{m=1}^{n-1} \frac{v_m \cdot \psi_n}{|v_m|^2} v_m. \end{aligned}$$

In principle this will produce a set of orthogonal vectors that should be close to the next solution. However, since we are removing larger and larger parts of the older solution vectors, they will start to have numeric errors quite quickly. The basis vectors are constructed so that the most recent solutions have the smallest error. The latest one is just normalized, the one before that is made orthogonal to just the previous one and so on. This way we keep at least the most important vectors.

Next we project the fermion matrix and the fermion field to this basis,

$$\begin{aligned} G_{nm} &= v_n M^\dagger M v_m \\ b_n &= v_n^\dagger \chi. \end{aligned}$$

Now we can solve equation 3.27,

$$G_{nm} a_m = b_n.$$

And finally project back to the original basis,

$$\psi_0 = \sum_m a_m v_m,$$

where ψ_0 is the chronological initial guess for the full solution.

The initial guess is often surprisingly close to the correct solution and the number of iterations in the conjugate gradient can be reduced significantly. The initial guess of course works best when the time step is small. It can reduce the computation time of a single time step by more than 90%. The downside is that the vectors the initial guess is constructed out of contain information about the previous states and this affects the balance requirement of a Markov chain. To ascertain detailed balance one can either demand greater accuracy from the conjugate gradient or reduce the step size. Both of these measures of course increase the computation time. Nevertheless we find the chronological initial guess often decreases computation time greatly.

3.5 Spectrum of SU(2) with Two Adjoint Fermions

In article [1] we have studied the mass spectrum of a lattice gauge model with two fermions interacting with the adjoint representation of an SU(2) gauge field. Since a conformal field cannot have a mass scale, all bound states in it should be massless. By studying how the masses run to zero with quark mass it should be possible to determine whether the model has a conformal fixed point. In the article we have mapped the phase structure of the model and measured the masses of several bound states and studied their running towards zero quark mass.

Since we are using Wilson-fermions and have broken the chiral symmetry explicitly, the fermion masses can receive additive quantum corrections. To simulate models with massless fermions we first need to find the critical hopping-parameter κ_c, where the true fermion mass is zero. We can measure the mass using the partial conservation of the axial current, the PCAC relation,

$$\frac{1}{2}(\partial_\mu^* + \partial_\mu) < A_\mu^a(x) O >= 2M < P^a(x) O >, \tag{3.28}$$

$$A_\mu^a(x) = \bar{\psi}(x)\gamma_\mu\gamma_5\frac{1}{2}\lambda^a\psi(x), \tag{3.29}$$

$$P^a(x) = \bar{\psi}(x)\gamma_5\frac{1}{2}\lambda^a\psi(x) \tag{3.30}$$

A_μ here is the axial current and P is the pseudo-axial current. The operator O can in principle be anything. One possible choice is to add a source fermion field χ to the time slice $x_0 = 0$, and use the pseudo-axial current of the source field

$$O^a = \sum_{\mathbf{y},\mathbf{z}} \bar{\chi}(0,\mathbf{y})\gamma_5\frac{1}{2}\lambda^a\chi(0,\mathbf{z}).$$

This should be strongly correlated to the pseudo-axial current in the bulk of the lattice, providing good signal.

Measuring the masses of bound states like mesons is actually rather straightforward on the lattice, even though it is very complicated in perturbation theory. The euclidean time propagators decay with energy, and the lowest energy state, the mass, can be measured from the long distance behavior. This can be seen simply by expanding the propagator in terms of energy states,

$$\begin{aligned}
\left\langle \Gamma(\tau)\Gamma^\dagger(0) \right\rangle &= \left\langle 0 \right| \Gamma(\tau)\Gamma^\dagger(0) \left| 0 \right\rangle = \left\langle 0 \right| e^{\hat{H}\tau}\Gamma(0)e^{-\hat{H}\tau}\Gamma^\dagger(0) \left| 0 \right\rangle \\
&= \sum_n \left\langle 0 \right| e^{\hat{H}\tau}\Gamma(0) \left| E_n \right\rangle \left\langle E_n \right| e^{-\hat{H}\tau}\Gamma^\dagger(0) \left| 0 \right\rangle \\
&= \sum_n \left\langle 0 \right| \Gamma(0) \left| E_n \right\rangle e^{-E_n\tau} \left\langle E_n \right| \Gamma^\dagger(0) \left| 0 \right\rangle \\
&= \sum_n e^{-E_n\tau} \left| \langle 0 | \Gamma(0) | E_n \rangle \right|^2 \\
&\approx Ae^{-m\tau}.
\end{aligned}$$

On the last line we have taken the time τ to be large compared to the lattice spacing and $1/m$, but small compared to the size of the lattice. To measure the mass of a bound state we need to construct an operator that overlaps with the state and fit the long distance behavior to an exponentially decaying function. At large distance the leading behavior is given by the smallest energy state of the operator, that is the mass of the lightest bound state it overlaps.

We found indications of a first order phase transition at large coupling. There is a sudden jump in the expectation value of both the quark mass and the plaquette observable,

$$P = \left\langle 1 - \frac{1}{N_C V} \sum_{x,\mu>\nu} \mathrm{Tr}(U_{\mu\nu}(x)) \right\rangle,$$

where $U_{\mu\nu}$ is the plaquette and V is the volume of the lattice. The plaquette is related to the field strength tensor. At the transition it jumps to a significantly smaller value. The phase transition is easily visible if we plot the plaquette as a function of κ, figure 3.2. The measurements were performed on a lattice with the size $L = 10$ in all directions.

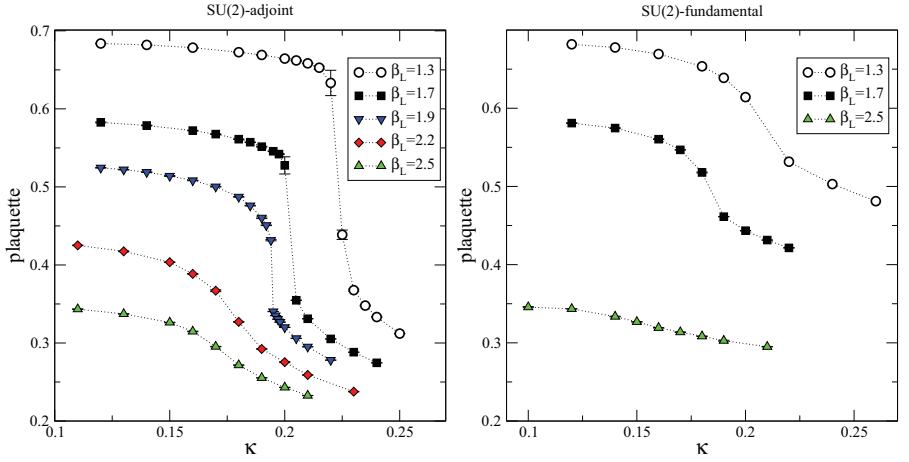

Figure 3.2: Plaquette expectation values as measured in article [1] at several values of the bare coupling. The values of the left panel were measured from SU(2) gauge theory with two adjoint fermions and the ones in the right panel with two fundamental fermions.

As we see on the left hand side in figure 3.2, in the model with fermions in the adjoint representation, the transition is abrupt when $\beta < 2$. The errors in measurements are large close to the transition and it is difficult to actually map the transition exactly. When $\beta > 2$ and the coupling is weaker, the transition is smoother and simulations seem to be reliable all the way trough it. The same change in the plaquette observable can be seen in the fundamental theory as well, on the right side in the plot, but it is not as drastic and does not limit simulations in the range of β that was studied.

The phase transition seems to be a lattice phenomenon. Since the quark mass in physical units, m/a, should be kept constant while approaching continuum, the lattice mass m must approach zero in the continuum limit. The mass however jumps at the transition and if it jumps from positive to negative values, there is no point where the mass is zero and therefore no continuum limit. There is a discontinuity between the continuum limit where the transition happens at negative mass and the continuum limit where it happens at positive mass. These two continuum models do not necessarily correspond to the same physical theory. To reach reliable continuum results, we must therefore stay at large enough β where the transition happens at negative quark mass.

Keeping this in mind we have studied the masses of the lightest pseudo scalar meson, the pion π, and the lightest vector meson ρ. In figure 3.3 we have plotted the masses as a function of the lattice quark mass $m = m_Q a$ from the PCAC relation 3.28. At larger couplings, $\beta \leq 1.9$, the behavior is compatible with chiral symmetry breaking. The pion mass approaches zero with like the square root of the quark mass. This is how the Goldstone boson of a broken chiral symmetry should behave. The vector meson on the other hand seems to tend to a finite mass, suggesting that there is a mass scale in the continuum model.

Below the expected critical coupling around $\beta = 2$, at values $\beta \geq 2.2$, the behavior changes. Both particles have almost degenerate masses and seem to be directly proportional to the quark mass. This kind of behavior is compatible with a model close to a conformal fixed point. With no other mass scale available the meson masses would be relative to the quark mass and tend to zero. The chiral symmetry breaking observed at larger couplings could well be a lattice artifact, since at these coupling we are above the bulk phase transition and do not necessarily describe a continuum limit. The seemingly conformal behavior at

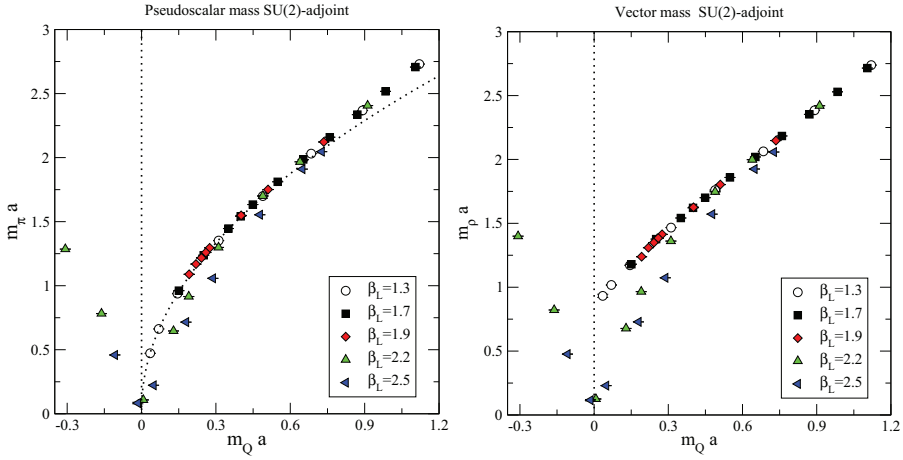

Figure 3.3: On the left: Pseudo scalar meson π mass with respect to the quark mass $m = m_Q a$. The dotted line is a fit $\propto \sqrt{m_Q}$ to measurements at $\beta_L \leq 1.9$ and $m = m_Q a \leq 0.5$. On the right: Vector meson ρ mass with respect to the lattice quark mass $m_Q a$.

smaller coupling could be the physical behavior of the model.

There is another interpretation, however. Similar behavior is observed in models with a true chiral symmetry breaking. At larger couplings the system is confined and the chiral symmetry breaking is visible. At smaller couplings, however, the lattice size is too small compared to the chiral condensate and the system seems to behave like a free, conformal theory.

Similar studies have been performed by other groups, reported in [19, 20, 21, 22, 23, 24, 25], with similar results. Even though the bulk transition and the chiral symmetry breaking seem to be lattice effects, and conformal behavior is observed, there is some reason to doubt this interpretation of our results. Similar effects can be observed in a model that certainly has a chiral symmetry breaking. Based on article [1], the SU(2) gauge theory with two adjoint fermions may well have a conformal fixed point, but there is no direct proof. To explore the conformality of the model directly we have turned to measurements of the running coupling and the β function.

Chapter 4

The Running Coupling and Discretization Errors

4.1 The Schrödinger Functional

For measuring the the strength of the interaction from lattice simulations we have used the Schrödinger Functional (SF) [26] method. It amounts to generating a background field in the simulated system and finding the interaction strength by varying the field and measuring the effect this has on the action of the system. Several other methods of measuring the coupling are used by other groups, many of which are variations of the SF method with improvements, such as the twisted Polyakov loop method [17], but some use different mechanisms, such as Wilson loops that describes the potential between two quarks.

The main problem with the Schrödinger Functional method is that discretization effects appear to first order in the lattice spacing. With for example the twisted Polyakov loop approach these effects appear only to second order in the lattice spacing and disappear faster in the continuum limit. The problem with the twisted Polyakov loop method is that the number of quark flavors is by construction restricted to a multiple of $2 \times N_c$, N_c being the number of colors in the model. The SF approach does not have this limitation, but one has to take care of the discretization effects.

The SF background field is created by fixing the gauge field at the boundaries of the lattice in time direction,

$$U_i(x_0 = 0) = U_0(\eta) = e^{-i\eta\lambda_3/L}, \tag{4.1}$$

$$U_i(x_0 = T) = U_T(\eta) = e^{-i(\pi-\eta)\lambda_3/L}. \tag{4.2}$$

At classical level, where the system is described by the minimum of the action, the field settles into a smooth interpolating field between the boundary values. For this classical background field, the variation of the action with respect to η is inversely proportional to the bare coupling,

$$\frac{dS_{cl}}{d\eta} = \frac{k}{g_0^2}.$$

The constant k depends on η and the size of the lattice.

Above two-loop level in perturbation theory there is no unique way to define the renormalized coupling. As long as other renormalized quantities are defined consistently, the only restriction is that it should agree with the classical value when the bare coupling is small. The SF coupling is defined analogously to the classical case, using the expectation value of

the derivative of the action,

$$\left\langle \frac{\partial S^{\text{cl.}}}{\partial \eta} \right\rangle = \frac{k}{g^2}. \tag{4.3}$$

Note that the classical coupling g_0 is actually just a parameter of the lattice field theory that appears in the action. It cannot be measured and has no direct physical interpretation. Any coupling that is measured will be some version of a renormalized coupling.

We should also set fermion fields at the time boundary and the simplest choice is to take $\psi(x_0 = 0) = \psi(x_0 = T) = 0$. The fermion part of the action goes to zero at the boundaries and does not depend on η. Only the gauge part contributes to the derivative and it is straightforward to calculate.

In the spacial direction the normal periodic boundary condition can be used. This amounts to wrapping the boundaries together into a cylinder, so that moving the distance L to any direction brings you back to the starting point, $x = x + L\hat{\mu}$. The tree-level gauge field should be constant in the spacial direction, so the only periodic choice is

$$U(x_i = L + 1) = U(x_i = 0).$$

The quark fields can have an extra phase,

$$\psi(x_i = L + 1) = e^{i\theta}\psi(x_i = 0), \;\; \bar{\psi}(x_i = L + 1) = e^{-i\theta}\bar{\psi}(x_i = 0). \tag{4.4}$$

The effect of the phase on simulation time was investigated in [27] for SU(3). In this case, choosing $\theta = \pi/5$ seems to regulate the low-lying fermion modes and make inverting the fermion matrix faster without affecting the coupling. Motivated by these studies we use $\theta = \pi/5$ when measuring the coupling and $\theta = 0$ otherwise, even though we use different models.

The SF coupling is intuitively related to the strength of the interaction, it has the correct classical limit and can be related to the $\overline{\text{MS}}$ coupling often used in perturbation theory. It is also directly connected to a distance scale, the distance between the time boundaries. This is useful in studying the scale dependence of the coupling, the β-function.

The observable in 4.3 is generally noisy and suffers from long correlation times. To get to a good accuracy, the simulations tend to be long and time-consuming, spanning typically a couple hundred thousand HMC trajectories. As the computing cost increases rapidly with the volume, the studies are limited to rather small lattice sizes, typically between $L = 6$ and $L = 16$.

In [28] the running of the SF coupling was studied in the SU(2) model with two adjoint fermions. The coupling was measured at several values of β with several lattice sizes. The results can be seen in figure 4.1. We are interested in the direction the coupling runs with the lattice size since change in the direction would indicate a fixed point. At small coupling the β-function is negative and the coupling increases with lattice size. At larger couplings the direction of the running changes and the β-function turns positive. There seems to be a zero of the β-function there between $g^2 = 2$ and $g^2 = 3$.

The lattice model seems to be conformal. On the other hand the results in figure 4.1 have large discretization errors. Even at smaller couplings, the results at $L = 4$ seem incompatible with the larger lattice sizes. When the direction of the running flips, the coupling is still running up at $L = 6$. Since the measurements at $L = 20$ have large errors and constrain the results only weakly, the conclusion is actually based on just two points, $L = 12$ and $L = 16$.

The measurements in article [28] clearly hint to the existence of a fixed point, at least one seems to exist in the lattice model, but the discretization errors prevent taking a reliable continuum limit from the results. The next step is to find a method for controlling the continuum limit and the discretization errors.

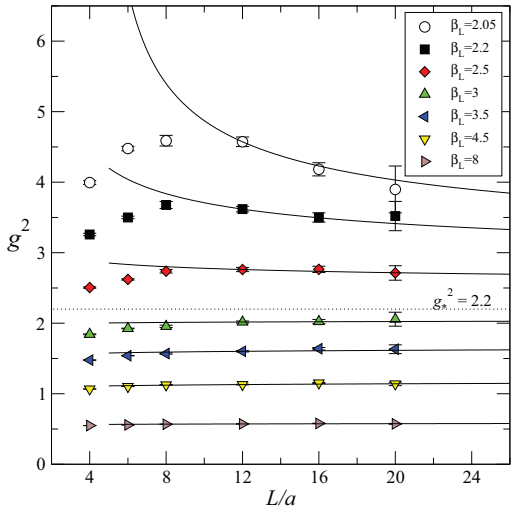

Figure 4.1:

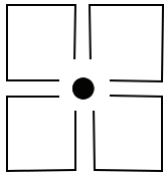

Figure 4.2: A diagrammatic representation of the clover term.

4.2 Symanzik Improvement

There are basically two approaches to improving a lattice model. Either one tries to find a model that describes the physical system as well as the old one but is faster to simulate, or a model that represents the physical continuum model more accurately already on smaller lattices, that is, has smaller discretization errors. There is a lot of freedom in choosing a lattice model, it only has to produce the correct continuum limit, and many possible improvements have been suggested.

In the Symanzik improvement method [29, 30] the action, or any operator that needs to be improved, is expanded in terms of the lattice spacing a. The leading terms are then cancelled by adding equal and opposite terms to the model. At the first order there is only one operators that can be added to the Wilson action without breaking any symmetries and that cannot be removed by normalizing the fields [31]. This is the Sheikholeslami-Wohlert or clover term

$$O_{SW} = a\bar{\psi}\sigma_{\mu\nu}F_{\mu\nu}\psi$$

We are now using the physical units, where a is not set to 1.

The clover operator connects the fermion fields ψ to the field strength tensor of the gauge field. The diagrammatic representation of the operator in figure 4.2 looks like a four leaf clover, the fermion fields are parallel transported around all possible plaquettes, ending at

the original position. $\sigma_{\mu\nu}$ is an antisymmetric product of the gamma-matrices,

$$\sigma_{\mu\nu} = \frac{i}{2}[\gamma_\mu, \gamma_\nu].$$

Adding this to the action with an arbitrary coefficient $c_{\rm sw}$ we get the fermion action

$$S_F = a^4 \sum_{\alpha=1}^{N_f/2} \sum_x \left[\bar{\psi}_\alpha(x)(iD + m_0)\psi_\alpha(x) + a c_{\rm sw} \bar{\psi}_\alpha(x) \frac{i}{4} \sigma_{\mu\nu} F_{\mu\nu}(x) \psi_\alpha(x) \right], \qquad (4.5)$$

where N_f is the number of fermion flavors. If we choose the coefficient $c_{\rm sw}$ properly as a function of β and N_f, all the first order discretization effects should disappear.

In article [2] we find the coefficient $c_{\rm sw}$ nonperturbatively for SU(2) with 2 flavors of fermions in the fundamental and adjoint representations and demonstrate that this removes a large part of the discretization errors present in the fermion mass. The method for finding the coefficient $c_{\rm sw}$ was used in reference [32] for studying QCD. To find the coefficient we measure the fermion mass using the PCAC relation in two different ways. With the Schrödinger functional boundary conditions, we measure the mass M with the source field at the lower boundary, as in equation 3.28. We also measure the mass M' with the source at the upper boundary, with the operator

$$O^a = \sum_{\mathbf{y},\mathbf{z}} \bar{\chi}(T, \mathbf{y}) \gamma_5 \frac{1}{2} \lambda^a \chi(T, \mathbf{z}).$$

Both of these measurements should give the same renormalized fermion mass in the continuum. The only difference is that in one the source field for the correlators is in the lower boundary and in the other it is on the upper boundary. The discretization errors in these measurements can be different, however, since the boundary condition are different. If there are no discretization errors, the value for $c_{\rm sw}$ is correct, the difference

$$dM(x_0) = M(x_0) - M'(x_0) \qquad (4.6)$$

should disappear. We can measure dM at a few different values of $c_{\rm sw}$ and find the point where $dM(x_0) = 0$ at some x_0.

For the model with fundamental fermions we used the same SF boundary condition as when measuring the coupling, given in 4.1, with $\eta = 0.25\pi$. We call these boundary conditions Abelian boundaries. With adjoint fermions, however, there is a complication. In the adjoint representation the boundary matrices become

$$\widetilde{U}_0(\eta) = \begin{pmatrix} \cos\left(\frac{a\eta}{2L}\right) & -\sin\left(\frac{a\eta}{2L}\right) & 0 \\ \sin\left(\frac{a\eta}{2L}\right) & \cos\left(\frac{a\eta}{2L}\right) & 0 \\ 0 & 0 & 1 \end{pmatrix},$$

$$\widetilde{U}_T(\eta) = \begin{pmatrix} \cos\left(\frac{a(\pi-\eta)}{2L}\right) & -\sin\left(\frac{a(\pi-\eta)}{2L}\right) & 0 \\ \sin\left(\frac{a(\pi-\eta)}{2L}\right) & \cos\left(\frac{a(\pi-\eta)}{2L}\right) & 0 \\ 0 & 0 & 1 \end{pmatrix}.$$

The third fermion color is not affected by the boundaries and therefore doesn't contribute to dM. At long distances the third color starts to dominate and the dM goes to zero regardless of the boundary matrices.

We see this figure 4.3. On the plot on the left we show the tree-level mass $M(x_0)$ in the model with fundamental fermions at two different values of $c_{\rm sw}$. There is a clear difference

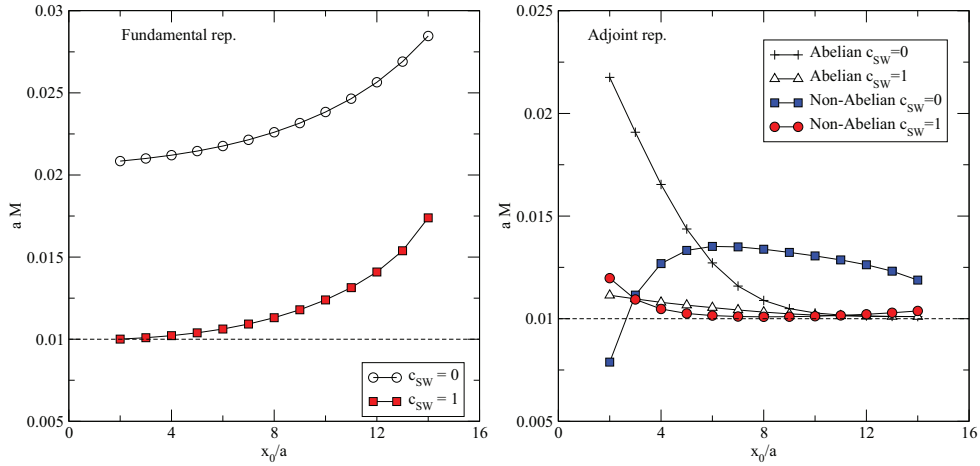

Figure 4.3: *Left:* Fermion masses $m(x_0) = aM(x_0)$ measured from the classical configuration with SF boundary conditions. The plot on the left side shows masses of fermions on the fundamental representation measured with the boundary conditions in 4.1 (Abelian). The plot on the right side shows masses of adjoint fermions measured using both the boundary conditions 4.1 (Abelian) and 4.7 (Non-Abelian). The bare mass is 0.01, and any difference from this is due to cutoff effects.

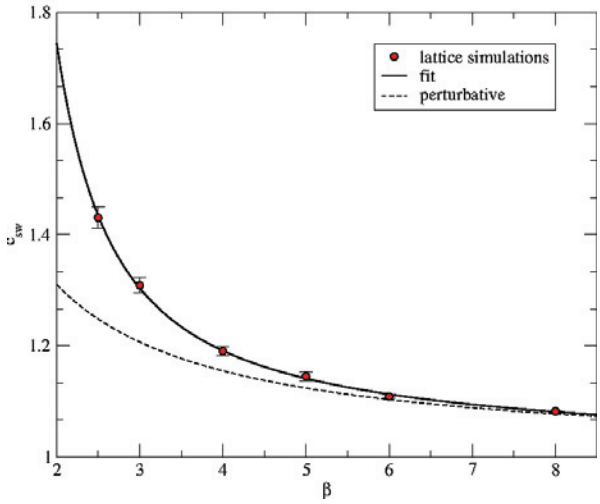

Figure 4.4: $c_{\rm sw}$ for two flavors of fundamental representation fermions. The solid line is the interpolating fit and the dashed line is the 1-loop perturbative value

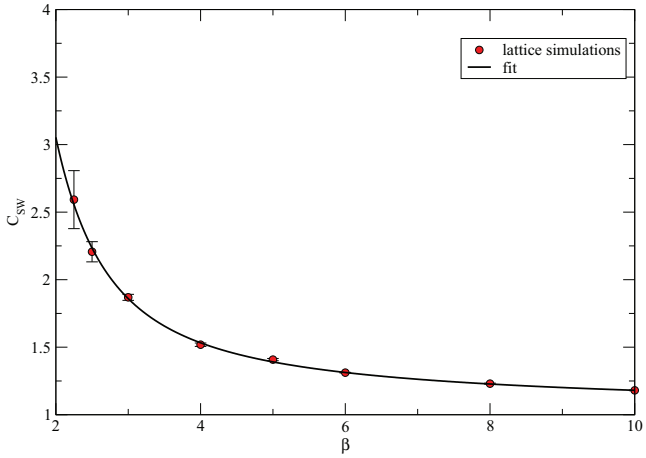

Figure 4.5: $c_{\rm sw}$ for two flavors of adjoint representation fermions, with the interpolating fit.

between the two cases. In the plot of the right we show the same for the model with adjoint fermions. There the difference in the mass between the two values of $c_{\rm sw}$ dissappears when x_0 is larger than 8.

We remedied the problem by using different, direction-dependent boundary conditions when measuring $c_{\rm sw}$ with adjoint fermions. The boundary matrices where chosen to be

$$U_i(x_0 = 0) = \exp\left(-i\frac{\pi}{2}\frac{a\lambda_i}{L}\right), \qquad (4.7)$$
$$U_i(x_0 = T) = I.$$

The new boundary conditions, dubbed Non-Abelian, produce a strong background field with a magnetic component in addition to the electric one. We do not use them to measure the coupling, but they are useful in measuring dM. In figure 4.3 we show also the fermion mass measured from the classical configurations produced by these boundary conditions. The difference between the unimproved case, $c_{\rm sw} = 0$, and the improved case, $c_{\rm sw} = 1$, remains visible also at larger distances.

Since the boundaries are fixed in the Schrödinger functional method and the Lorentz symmetry is broken, there are two other terms that can be added at the boundary,

$$\delta S_F = a(\tilde{c}_t - 1)\sum_x \frac{1}{a}\bar{\psi}(x)\psi(x)(\delta(x_0 - a) + \delta(x_0 - (L - a)) \text{ and}$$
$$\delta S_G = a(c_t - 1)\frac{\beta_L}{4}\sum_{x,\mu,\nu} \mathrm{tr}(1 - U_{\mu,\nu}(x))(\delta(x_0 - a) + \delta(x_0 - (L - a)).$$

These are basically corrections to the bare coupling and mass, but present only at the time boundaries. They are controlled by the parameters $\tilde{c}_t$ and c_t and these were calculated to first order in perturbation theory in article [2].

Actually only the c_t term has an effect on the SF coupling to the first order. The $\tilde{c}_t$ term renormalizes the fermion mass and only affect the coupling in higher orders in perturbation theory. We have included it for consistency, since we also measured the position of the critical line $\kappa = \kappa_c$, where the fermion mass is zero. Similarly, for consistency, one should

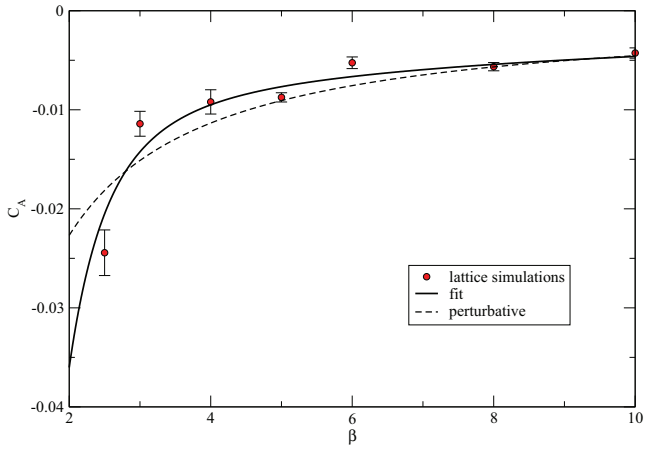

Figure 4.6: c_A for two flavors of adjoint fermions. The solid line is the interpolating fit and the dashed line is the 1-loop perturbative value

also improve the axial current A_μ used to measure the fermion mass. The improved version is

$$A^a_{I,\mu} = A^a_\mu + a\, c_A\, \frac{1}{2}(\partial^*_\mu + \partial_\mu) P^a.$$

We also measured the coefficient c_A nonperturbatively, using the effect of the space-like boundary condition in equation 4.4 on the fermion mass.

We measured the coefficient $c_{\rm sw}$ at few values of β. For use in simulations at different values of β, we found an interpolating function for the results. The interpolating function for $c_{\rm sw}$ shown in figures 4.4 and 4.5. The results and the interpolating function for c_A is shown in figure 4.6.

We found that the non-perturbative values for the improvement coefficients seem to diverge around $\beta = 2$. It seems that beyond this point the discretization effects start to dominate and simulations of the improved model become impossible. This gives validity to our earlier result, that the discretization errors grow large at smaller β. With adjoint fermions this happens before the fixed point, making it impossible to verify its existence using the purely Symanzik improved action.

4.3 The Continuum Limit

In order to take the continuum limit we have to quantify the running independently at several lattice sizes. The continuum limit is taken by taking the lattice size to infinity while keeping physical quantities, such as the measured coupling, constant. The running of the coupling can be quantified by measuring it with two different lattice sizes, for example L^4 and $(2L)^4$. The change is then encoded in the step-scaling function [33], which describes the change of the coupling when the physical size of the system is doubled,

$$\Sigma(u, L) = g^2(g_0, 2L)\big|_{g^2(g_0,L)=u}\,, \tag{4.8}$$

$$\sigma(u) = \lim_{L\to\infty} \Sigma(u, L). \tag{4.9}$$

Σ is the lattice version and σ the continuum limit.

The continuum step scaling function is calculated from the values of Σ at several lattice sizes, keeping the coupling g^2 constant, and taking the limit $a \to 0$. Since the simulations are very time-consuming it is not practical to find bare couplings so that g^2 is constant at all lattice sizes. Instead the measured values of g^2 can be fitted to an interpolating function, which is then used to calculate Σ at different lattice sizes.

In the previous sections we quantified the running using the β-function, which is a more natural choice in perturbation theory. The step-scaling function and the β-function are of course related. The β-function describes the change of the coupling with an infinitesimal change of the energy scale and the step-scaling function with the doubling of the distance scale. By letting the coupling run from a distance scale to double the scale we get

$$\int_{g^2}^{\sigma(g^2)} \frac{dx}{2\sqrt{x}\beta(\sqrt{x})} = -\int_{L}^{2L} \frac{dL}{L} = -\ln(2) \tag{4.10}$$

Generally speaking the relation is a bit complicated, but we are mostly interested in finding a fixed point, where the coupling doesn't run and the β-function has a zero. Close to a fixed point, where $\beta(g)$ is small, we can expand the integral in 4.10 to get

$$\beta(g) \approx \beta^*(g) = \frac{g}{\log(2)} \left(1 - \frac{\sigma(g^2)}{g^2}\right). \tag{4.11}$$

As one might expect, the zero of the β-function corresponds to $\sigma(u) = u$, where the coupling does not change with the length scale. The approximation is exact only when $\beta = 0$, but is generally quite good in the vicinity of a fixed point.

This method was used in [34, 35, 36, 37] to study SU(2)-models with adjoint or fundamental fermions with unimproved Wilson fermions. A fixed point is seen in the lattice results in both cases, but in the continuum limit the systematic errors are too large to make rigorous conclusions. We have used the method to find the continuum limit of the step scaling function in [3] using Symanzik improved Wilson fermions with perturbative values for the improvement coefficients.

For the model to be conformal we must simulate with massless fermions. To find the value of κ where the fermion mass is zero, we have measured the mass from the PCAC relation in equation 3.28 using a few values of κ for each bare coupling. Using the largest lattice size, $L = 16$, we have measured the correlation functions at the middle time slice, $x_0 = L/2$ and interpolated to find $\kappa = \kappa_c$ where the mass is zero. The simulations needed to find the mass are relatively short and usually have around 500 trajectories.

We have used the jackknife blocking method in our analysis, since it allows to perform complicated operations on the data and find the statistical error of the results in a straightforward way. The whole data set is divided into around 80 jackknife blocks, the whole analysis is done to each block separately, and the error is calculated from the distribution of the results. We go trough the whole process including the continuum limit for each jackknife block.

4.4 SU(2) with 4, 6 and 10 fermions

In article [3] we have studied the behavior of SU(2) with 4, 6 and 10 fermions using the perturbative value of c_{sw}. In the model with 10 fermions this seems to be a surprisingly good choice for c_{sw}. We noticed that at large coupling the discretization effect dM is actually rather small. At large coupling the non-perturbative value for c_{sw} seems depend on the number of fermion flavors rather strongly.

The most interesting case in the article is the one with 6 fermions, since it is close to the lower limit of the conformal window. The cases with 4 and 10 fermions are good benchmarks

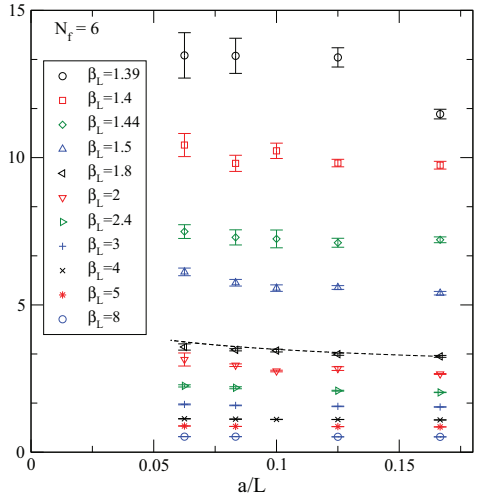

Figure 4.7: The measured values of g^2 against a/L with 6 flavours of fermions. The black dashed line gives an example of the running in 2-loop perturbation theory.

for the method, since the 4 fermion model is clearly below the conformal window and the 10 fermion model is clearly inside it. In both cases the results of the simulations are as expected, as we can see in figures 4.8 and 4.10.

In the four fermion model the step scaling function becomes clearly larger than one already at rather small couplings. The measured value follows the perturbative one at smaller coupling and seems to be slightly larger at large coupling. In the ten fermion model the step scaling function becomes clearly negative around $g^2 = 2.5$. Since it is positive at very small couplings, where it follows perturbation theory, there has to be a fixed point. The exact location of the fixed point remains hard to discern as the running is extremely slow at all values of the coupling below $g^2 = 2.5$. In this case the step scaling function seems to have a smaller value than the perturbative expansion already at rather small coupling.

The main conclusion that can be drawn from our measurements of the six fermion model is that the fixed point observed in [35] at around $g^2 = 4$ is either moved to much larger coupling or not present. The continuum extrapolation seems to follow the perturbative line quite well to large coupling and diverges from it abruptly at $g^2 = 8$. The continuum extrapolation is of course highly questionable already at $g^2 = 6$, where it clearly diverges from the $L = 8$ result. The drastic change the behavior around $g^2 = 8$ is caused by one measurement, the value of g^2 measured with $L = 6$ and $\beta = 1.39$ is clearly different from the other measurements at the same β. It seems that even though the results are good to a large coupling, the fixed point, if one exists, is still hidden by discretization errors.

4.5 Hypercubic Smearing

To remedy the problem of discretization errors diverging with large coupling we have implemented smearing of the fermion part of the action. The general idea of smearing is to reduce the fluctuations of the gauge field to bring it closer to the tree-level field. This is done by replacing gauge matrices in the action with an average of a group of paths. There are several ways to take the average and to choose the paths taken. In NHYP smearing, used in similar calculation in [38], the idea is to stay within a hypercube and use a differentiable

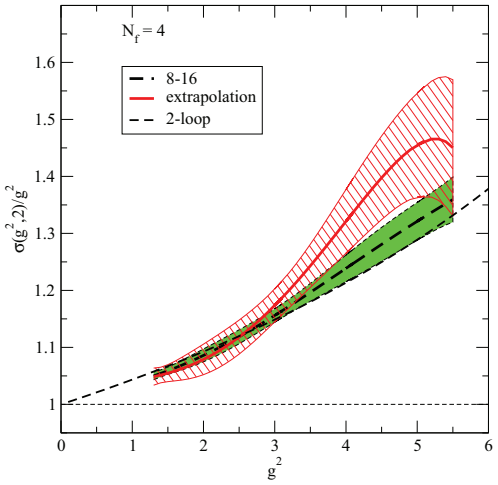

Figure 4.8: The normalized step scaling function $\sigma(g^2)/g^2$ with 4 fermions as in article [3]. The red line corresponds to the continuum extrapolation and the hashed band to the statistical error. The thick dashed line with the green error band corresponds to the measurements on the largest lattice $L = 8$. The thin dashed line is the 2-loop perturbative value.

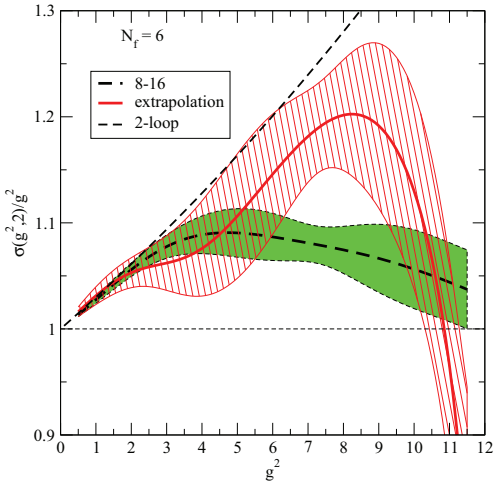

Figure 4.9: The normalized continuum step scaling function $\sigma(g^2)/g^2$ with 6 fermions as in article [3].

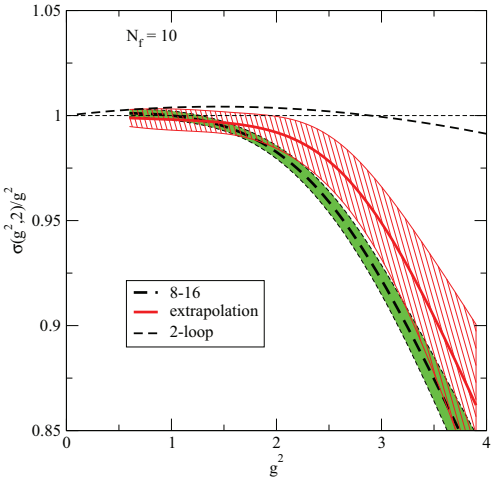

Figure 4.10: The normalized continuum step scaling function $\sigma(g^2)/g^2$ with 10 fermions as in article [3].

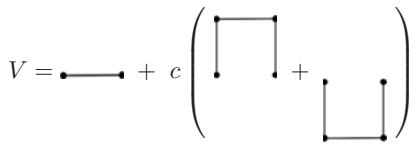

Figure 4.11: The link and the staples summed together in a two-dimensional lattice.

normalization of the sum of the paths that projects it into a U(N_C) matrix.

Smearing takes the model closer to the tree-level model and should remove a part of the discretization effects. In [38] it was found that replacing gauge links in the fermion action with NHYP smeared links enables simulations at larger bare coupling. Discretization errors remain small at larger couplings, which is evident from the fact that the clover coefficient stays close to the tree-level value $c_{\rm sw} = 1$. We have found similar results with adjoint SU(2) and are studying both adjoint SU(2) and SU(3) using perturbative order a improvement in addition to hypercubic smearing.

A general hypercubic smearing consists of three consecutive smearing steps. First we add together all possible staples, paths of three links connected to the endpoints of the smeared link, as shown in figure 4.11. The product is then normalized and the steps are repeated three times, taking only staples that are orthogonal to the staples that are already included. This ensures that the effect of the smearing stays withing a single hypercube and therefore within a clearly restricted physical volume.

The steps in a general hypercubic smearing are given by

$$\begin{aligned}
V_{x,\mu} &= \mathrm{Proj}\left(\Lambda_{\mathrm{x},\mu}, \mathrm{U}_{\mathrm{x},\mu}\right) \\
\Lambda_{x,\mu} &= \frac{\alpha_1}{6} \sum_{\pm\nu\neq\mu} \tilde{V}_{x,\nu;\mu} \tilde{V}_{x+\hat{\nu},\mu;\nu} \tilde{V}^{\dagger}_{x+\hat{\mu},\nu;\mu} \qquad (4.12) \\
\tilde{V}_{x,\mu;\nu} &= \mathrm{Proj}\left(\Lambda_{\mathrm{x},\mu;\nu}, \mathrm{U}_{\mathrm{x},\mu}\right) \\
\tilde{\Lambda}_{x,\mu;\nu} &= \frac{\alpha_2}{4} \sum_{\pm\rho\neq\mu,\nu} \overline{V}_{x,\rho;\nu,\mu} \overline{V}_{x+\hat{\rho},\mu;\nu,\rho} \overline{V}^{\dagger}_{x+\hat{\mu},\rho;\mu,\nu} \\
\overline{V}_{x,\mu;\nu,\rho} &= \mathrm{Proj}\left(\overline{\Lambda}_{\mathrm{x},\mu;\nu,\rho}, \mathrm{U}_{\mathrm{x},\mu}\right) \\
\overline{\Lambda}_{x,\mu;\nu,\rho} &= \frac{\alpha_3}{2} \sum_{\pm\eta\neq\mu,\nu,\rho} U_{x,\eta} U_{x+\hat{\eta},\mu} U^{\dagger}_{x+\hat{\mu},\eta}. \qquad (4.13)
\end{aligned}$$

For our implementation of NHYP smearing we have chosen the coefficients to be $\alpha_1 = 2.333$, $\alpha_2 = 1.5$ and $\alpha_3 = .4285$. The value for α_1 was found in [39] by minimizing the plaquette observable. The other two are tree-level values [40]. The normalization operator used in NHYP smearing is defined as

$$\mathrm{Proj}(\Lambda, \mathrm{U}) = \frac{\mathrm{M}}{\sqrt{\mathrm{M}^{\dagger}\mathrm{M}}}, \quad \mathrm{M} = \mathrm{U} + \Lambda.$$

The square root could be defined to be any matrix $S = \sqrt{M}$ that has the property $S \cdot S = M$, but since we need to calculate the derivative of the smeared link for the fermion force in the HMC algorithm, we should work out a differentiable definition. If D is a matrix that diagonalizes M, that is

$$D^{\dagger} M D = \begin{pmatrix} g_1 & 0 & \cdots \\ 0 & g_2 & \cdots \\ \vdots & \vdots & \ddots \end{pmatrix},$$

we define the square root to be

$$\sqrt{M} = D \begin{pmatrix} \sqrt{g_1} & 0 & \cdots \\ 0 & \sqrt{g_2} & \cdots \\ \vdots & \vdots & \ddots \end{pmatrix} D^{\dagger}$$

We first project the matrix to a space where it's diagonal, then take the square root and project it back. This square root can be expanded in terms of traces of the matrix,

$$\frac{1}{\sqrt{M}} = f_0 + f_1 M + \cdots + f_{N_C} * M^{N_C}, \qquad (4.14)$$

The coefficients f are functions of the traces of powers of M and are found by solving the equation

$$D^{\dagger} \frac{1}{\sqrt{M}} D = \begin{pmatrix} \sqrt{g_1} & 0 & \cdots \\ 0 & \sqrt{g_2} & \cdots \\ \vdots & \vdots & \ddots \end{pmatrix} = f_0 + f_1 \begin{pmatrix} g_1 & 0 & \cdots \\ 0 & g_2 & \cdots \\ \vdots & \vdots & \ddots \end{pmatrix} + f_2 \begin{pmatrix} g_1^2 & 0 & \cdots \\ 0 & g_2^2 & \cdots \\ \vdots & \vdots & \ddots \end{pmatrix} + \cdots$$

and noticing that $\mathrm{Tr}\,(M^n) = g_1^n + g_2^n + \cdots$. The derivative of this form can be worked out for $N_C = 2$ and 3.

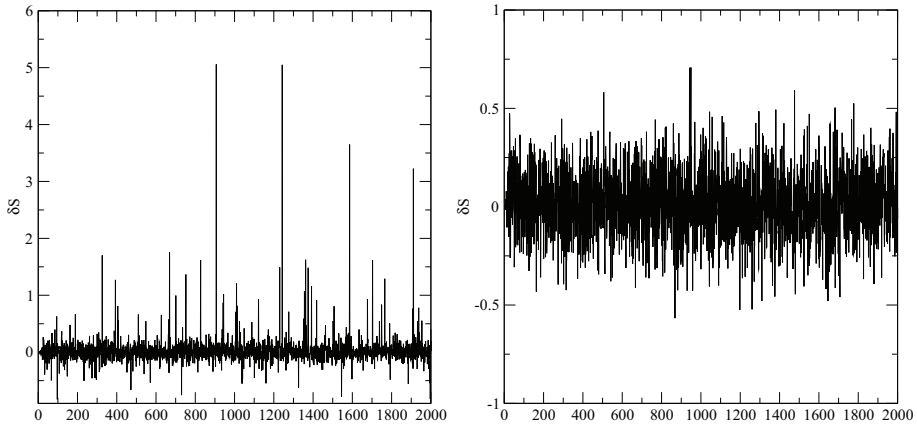

Figure 4.12: The change in action after each HMC trajectory, on the left using NHYP links for fermions and on the right using HEX links. The HMC parameters were chosen so that both simulations have the acceptance rate of approximately 90%.

While the NHYP smearing smooths the gauge field very effectively, we have noticed that it has a negative effect on the stability of the HMC trajectory when the coupling is large. The gauge matrices have large fluctuations and the sum of staples can sometimes be close to zero. Small fluctuation around zero then become large differences in the normalized matrix, producing large numerical errors in the derivative of the smeared link. This translates into large errors in the force term in the HMC trajectory.

The errors are seen as spikes in the change of the action δS during the HMC trajectory, as seen in a simulation history of δS on the left side of figure 4.12. When the spikes happen only occasionally they do not affect the acceptance rate of the HMC algorithm, but the detailed balance condition may holds. It is restored when the step size of the trajectory is very small, but this would make long simulations unfeasible.

This problem does not exist in exponential or stout smearing, where the smearing is done in the algebra of the SU(N) group. One calculates the sum of plaquettes that include a particular link and takes the traceless antihermitean part. This is interpreted as a matrix in the algebra of the SU group, and exponentiating it produces an SU(N) matrix. The smeared link is the product of this exponent and the original link.

The hypercubic stout or exponential smearing, HEX, has been studied in [41, 39] as an aid in simulating QCD with physical parameters. Our implementation of the HEX smearing consists of the three steps in the hypercubic smearing 4.13 with the parameters $\alpha_1 = 0.78$, $\alpha_2 = 0.61$ and $\alpha_3 = 0.35$. The projection is given by

$$\begin{aligned} &\mathrm{Proj}(\Lambda, \mathrm{U}) = \mathrm{e}^{-\mathrm{M}}\mathrm{U}, \\ &M = \Omega - \Omega^\dagger - \mathrm{Tr}\,[\Omega - \Omega^\dagger], \quad \Omega = \Lambda U^\dagger. \end{aligned}$$

The exponentiation can be written in a differentiable form similar to that in equation 4.14,

$$e^{-M} = f_0 + f_1 M + \cdots + f_{N_C} * M^{N_C}, \tag{4.15}$$

where the coefficients f can be worked out as function of traces, just as with the square root in NHYP smearing.

When the sum of the staples is close to zero, the exponentiation gives the unit matrix. The projection is analytic and continuous close to zero and there is no problem arising from

the differentiation at large coupling. The extreme spikes in the integration error are not present in the simulation history for with HEX smearing, on the right-hand side of figure 4.12. Both simulations are of the SU(2) gauge theory with 6 fundamental fermions. The lattice size is $L = 8$ and the bare coupling is chosen so that the renormalized couplings are close to each other. In the NHYP simulation we have used $\beta = 1.5$ and the SF coupling is $g^{-2} = 0.17(2)$. In the HEX simulation $\beta = 1.4$ and the SF coupling $g^{-2} = 0.13(3)$. The renormalized mass is tuned to zero and the size of the HMC integration step is chosen so that the acceptance rate is close to 93%.

Otherwise HEX smearing behaves similarly to NHYP smearing. The SF coupling seems to be slightly closer to the tree-level value and the plaquette expectation value slightly further away from it. In the discussed simulation the smeared space-like plaquette has the value 0.07677(7) in the NHYP case and 0.1096(2) in the HEX case. Most importantly the improvement parameter c_{sw} remains at its tree-level value $c_{\mathrm{sw}} = 1$. We have measured the discretization error dM in equation 4.6 in fundamental and adjoint SU(2) and it seems to have a zero close to $c_{\mathrm{sw}} = 1$, even at rather large couplings. The maximum value of c_{sw} we have measured in these models is $c_{\mathrm{sw}} = 1.1$.

The downside is that we do not have perturbative results with fermions beyond tree-level. In continuum, the effect of the smearing dissappears and the results are the same, but the discretization effects are different. We can, nevertheless, use Symanzik improvement to the first order in a and g^2, but only for the SF-coupling. The first order perturbative value of c_t is calculated from the interaction between fermions and the tree-level gague field, which remains unchanged. The other improvement coefficients can be kept at their tree-level values. Extending the improvement to other measurable quantities would require us to extend perturbation theory to the smeared links.

4.6 Smearing in the Gauge Action

In models with Wilson fermions there is a nonphysical phase transition when the fermion mass is large. The transition is characterized by a sudden change in both the plaquette expectation value and fermion mass. In the unphysical phase both are significantly larger than in the physical phase. We have found examples of the transition, for example, in unimproved SU(2) and in improved SU(2) and SU(3) with two adjoint fermions. The unphysical phase could be related to the Aoki phase in QCD where the flavor symmetry is spontaneously broken.

We show this transition for example in figure 3.2. At small coupling the transition is smooth and takes place at large bare mass, or small κ. As the coupling is increased it moves toward larger κ. When the transition line is close to the critical line κ_c, where the fermion mass is zero, simulations with massless fermions are no longer possible. If this happens before the conformal fixed point, the conformality of the model cannot be established.

The problem was studied in [42] in models with fermions the sextet representations of SU(3). It was alleviated by using a mixed gauge action, where a part of the gauge action uses the same smeared links as the fermions, in the sextet representation. I have studied the problem using adjoint SU(2) with a mixed gauge action, but using smeared links in the fundamental representation. The action is given by

$$S_G = (1 - c_g)\frac{\beta_L}{4} \sum_{x,\mu\neq\nu} \mathrm{Tr}\,(1 - U_{\mu\nu}(x)) + c_g \frac{\beta_L}{4} \sum_{x,\mu\neq\nu} \mathrm{Tr}\,(1 - V_{\mu\nu}(x)).$$

Here $U_{\mu\nu}$ is a plaquette constructed out of normal thin links and $V_{\mu\nu}$ is one constructed out of NHYP or HEX smeared links. In continuum the plaquettes are the same and the action is reduced to the normal plaquette action. The improvement coefficient c_g can in principle be chosen arbitrarily, as it does not change the action at the first order in a.

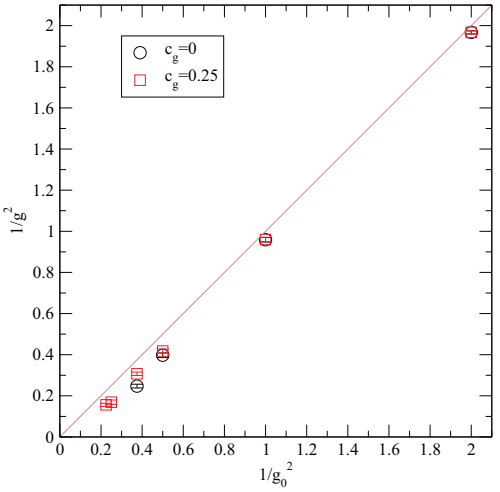

Figure 4.13: The coupling measured with and without smearing in the gauge action in SU(2) with 2 adjoint fermions. The highest value I was able to reach without the smearing is at $g^2 = 4.0(2)$. With smearing in the gauge action I was able to reach at least $g^2 = 6.4(3)$. The gray line represents the tree-level value $g^2 = g_0^2$.

In figure 4.13 I show the SF-couplings measured from a lattice with $L = 6$ in the SU(2) model with two adjoint fermions, both with HYPN mixed gauge action and without it. Without the gauge improvement the phase transition line crosses the critical line between $\beta = 1.5$ and $\beta = 1.1$. The highest value for the coupling I was able to reach was $g^2 = 4.0(2)$. With the gauge improvement the transition was not visible at the studied parameter range and I was able to reach at least $g^2 = 6.4(3)$.

As with NHYP smearing, using a mixed gauge action with HEX smearing seems to push the point where the critical line and the unphysical phase transition meet to a larger bare coupling and allow zero mass simulations at larger couplings. In figure 4.14 we see the phase transition in the model without the mixed action. With the gauge mixing parameter $c_g = 0.25$ the transition is not visible. Both simulations were performed with $\beta = 1.1$ with tree-level improvement and HEX smearing in the fermion action.

It seems evident that Symanzik improvement with HEX smeared fermion action and mixed gauge action enable simulations at much larger coupling than before, while keeping the discretization effects small. Tree-level improvement seems adequate to a rather large coupling and in the region we have studied the non-perturbative value of c_{sw} remains under control, growing only to around $c_{\mathrm{sw}} = 1.1$. Since HEX smearing is stable at large coupling it seems to be the practical choice for mapping the lower limit of the conformal window.

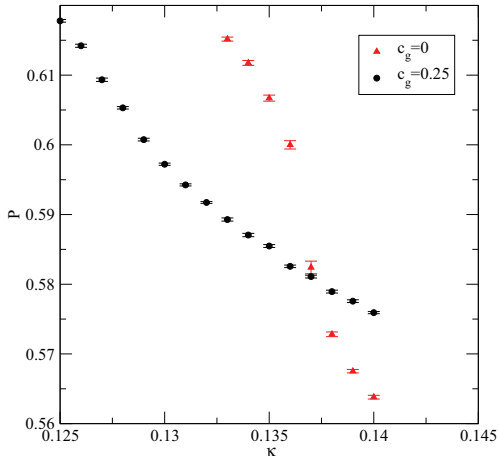

Figure 4.14: The expectation value of the plaquette observable in HEX smeared SU(2) with 6 fermions in the fundamental representation. The red data points were obtained without the mixed gauge action and the black ones with it. There is a clear transition in the values of the plaquette in the first case and the zero fermion mass within the transition, between $\kappa = 0.137$ and $\kappa = 0.138$. In the second case the phase transition is not clearly visible and the zero fermion mass is found between $\kappa = 0.133$ and $\kappa = 0.134$.

Chapter 5

Conclusions and Outlook

Non-Abelian gauge theories form the basis of our current understanding of the world at small length scales. Knowledge of the phase structure and strong coupling dynamics of these models is important in understanding and extending the Standard Model of particle physics. Conformal field theories, where the coupling runs to a constant at large energies, could be useful in explaining the masses of Standard Model particles trough the technicolor mechanism. This, however, requires us to understand the non-perturbative dynamics of these models.

Mapping the lower limit of the conformal window has turned out to be a significant challenge to the non-perturbative methods of studying these models. In some of the simplest models close to the lower limit the noisiness of the observables and the large dependence of the results on discretization effects has so far made it impossible to unambiguously distinguish between conformal and chirally broken behavior in the infrared part of the energy spectrum.

We have studied the phase structure of SU(2) models with fermions in fundamental and adjoint representations. In our first unimproved results we saw possible evidence of a conformal fixed point, but found that the discretization effects were too large to take an accurate continuum limit. Other groups have studied several models and come to similar conclusions. Close to the lower limit of the conformal window, where the fixed point is at a very large coupling, the discretization effects start to dominate the results before the fixed point is reached, making it impossible to find a continuum limit for the results.

To ameliorate the discretization effects we have studied methods of improving the lattice model and the effects of the improvement on the coupling defined trough the Schrödinger Functional method. We saw from the non-perturbative behavior of the improvement coefficient c_{sw} that the discretization effects grow large before the critical coupling is reached. We have found that the results from the improved models were different from the unimproved ones, showing that the discretization errors affected the results strongly. In the case of SU(2) with six fundamental fermions, we were unable to establish whether models is conformal or not, as the simulations became extremely slow at large coupling and the discretization errors started to affect the results.

The problem can be alleviated using smeared links in the fermion and gauge parts of the action. I have studied these improvements and their effect on the running coupling in both SU(2) with adjoint and fundamental fermions. Using HEX smearing it is possible to measure significantly larger values of the running coupling than with pure Symanzik improvement. We can now proceed to use this optimized, HEX smeared and Symanzik improved, action to map the β-functions and phase structures of these models and possibly establish the conformality of SU(2) with 6 fermion flavors.

Bibliography

[1] A. J. Hietanen, J. Rantaharju, K. Rummukainen and K. Tuominen, JHEP **0905**, 025 (2009) [arXiv:0812.1467 [hep-lat]].

[2] T. Karavirta, A. Mykkanen, J. Rantaharju, K. Rummukainen and K. Tuominen, JHEP **1106**, 061 (2011) [arXiv:1101.0154 [hep-lat]].

[3] T. Karavirta, J. Rantaharju, K. Rummukainen and K. Tuominen, arXiv:1201.2037 [hep-lat].

[4] S. Weinberg, Phys. Rev. D **19**, 1277 (1979).

[5] S. Weinberg, Phys. Rev. D **13**, 974 (1976).

[6] L. Susskind, Phys. Rev. D **20**, 2619 (1979).

[7] S. Dimopoulos and L. Susskind, Nucl. Phys. B **155**, 237 (1979).

[8] E. Eichten and K. D. Lane, Phys. Lett. B **90**, 125 (1980).

[9] C. N. Yang and R. L. Mills, Phys. Rev. **96**, 191 (1954).

[10] J. M. Cornwall, Phys. Rev. D **10**, 500 (1974).

[11] T. W. Appelquist, D. Karabali and L. C. R. Wijewardhana, Phys. Rev. Lett. **57**, 957 (1986).

[12] I.P. Omelyan, I.M. Mryglod and R. Folk, Computer Physics Communications, Volume 151, Issue 3, 1 April 2003.

[13] T. Takaishi and P. de Forcrand, Phys. Rev. E **73**, 036706 (2006) [arXiv:hep-lat/0505020].

[14] R. C. Brower, T. Ivanenko, A. R. Levi and K. N. Orginos, Nucl. Phys. B **484**, 353 (1997) [arXiv:hep-lat/9509012].

[15] A. D. Kennedy, I. Horvath and S. Sint, Nucl. Phys. Proc. Suppl. **73**, 834 (1999) [hep-lat/9809092].

[16] M. Hasenbusch and K. Jansen, Nucl. Phys. Proc. Suppl. **106**, 1076 (2002) [hep-lat/0110180].

[17] G. M. de Divitiis, R. Frezzotti, M. Guagnelli and R. Petronzio, Nucl. Phys. B **422** (1994) 382 [hep-lat/9312085].

[18] T. van Ritbergen, J. A. M. Vermaseren and S. A. Larin, Phys. Lett. B **400** (1997) 379 [hep-ph/9701390].

[19] S. Catterall and F. Sannino, Phys. Rev. D **76**, 034504 (2007) [arXiv:0705.1664 [hep-lat]].

[20] L. Del Debbio, A. Patella and C. Pica, Phys. Rev. D **81**, 094503 (2010) [arXiv:0805.2058 [hep-lat]].

[21] S. Catterall, J. Giedt, F. Sannino and J. Schneible, JHEP **0811**, 009 (2008) [arXiv:0807.0792 [hep-lat]].

[22] L. Del Debbio, B. Lucini, A. Patella, C. Pica and A. Rago, Phys. Rev. D **80**, 074507 (2009) [arXiv:0907.3896 [hep-lat]].

[23] L. Del Debbio, B. Lucini, A. Patella, C. Pica and A. Rago, Phys. Rev. D **82**, 014510 (2010) [arXiv:1004.3206 [hep-lat]].

[24] L. Del Debbio, B. Lucini, A. Patella, C. Pica and A. Rago, Phys. Rev. D **82**, 014509 (2010) [arXiv:1004.3197 [hep-lat]].

[25] F. Bursa *et al.*, Phys. Rev. D **84**, 034506 (2011) [arXiv:1104.4301 [hep-lat]].

[26] M. Luscher, R. Narayanan, P. Weisz and U. Wolff, Nucl. Phys. B **384**, 168 (1992) [arXiv:hep-lat/9207009].

[27] S. Sint and R. Sommer, Nucl. Phys. B **465**, 71 (1996) [arXiv:hep-lat/9508012].

[28] A. J. Hietanen, K. Rummukainen and K. Tuominen, Phys. Rev. D **80**, 094504 (2009) [arXiv:0904.0864 [hep-lat]].

[29] K. Symanzik, Nucl. Phys. B **226** (1983) 205.

[30] K. Symanzik, Nucl. Phys. B **226** (1983) 187.

[31] B. Sheikholeslami and R. Wohlert, Nucl. Phys. B **259** (1985) 572.

[32] M. Luscher, S. Sint, R. Sommer, P. Weisz and U. Wolff, Nucl. Phys. B **491** (1997) 323 [hep-lat/9609035].

[33] T. Appelquist, G. T. Fleming and E. T. Neil, Phys. Rev. D **79**, 076010 (2009) [arXiv:0901.3766 [hep-ph]].

[34] F. Bursa, L. Del Debbio, L. Keegan, C. Pica and T. Pickup, Phys. Rev. D **81**, 014505 (2010) [arXiv:0910.4535 [hep-ph]].

[35] F. Bursa, L. Del Debbio, L. Keegan, C. Pica and T. Pickup, Phys. Lett. B **696**, 374 (2011) [arXiv:1007.3067 [hep-ph]].

[36] H. Ohki *et al.*, PoS **LATTICE2010**, 066 (2010) [arXiv:1011.0373 [hep-lat]].

[37] G. Voronov *et al.* (Lattice strong dynamics collaboration): *Lattice Study of the Conformal Window in Two-Color Yang-Mills Theory*, Talk at LATTICE 2011, Squaw Valley, July 12 2011.

[38] T. DeGrand, Y. Shamir and B. Svetitsky, Phys. Rev. D **83**, 074507 (2011) [arXiv:1102.2843 [hep-lat]].

[39] A. Hasenfratz, R. Hoffmann and S. Schaefer, JHEP **0705**, 029 (2007) [arXiv:hep-lat/0702028].

[40] A. Hasenfratz and F. Knechtli, Phys. Rev. D **64**, 034504 (2001) [arXiv:hep-lat/0103029].

[41] S. Durr *et al.*, JHEP **1108**, 148 (2011) [arXiv:1011.2711 [hep-lat]].

[42] T. DeGrand, Y. Shamir and B. Svetitsky, PoS **LATTICE2011**, 060 (2011) [arXiv:1110.6845 [hep-lat]].